

Article

Development of a novel odd Weibull-half logistic distribution: Mathematical properties and applications

G. K. Musa¹, Ibrahim Adamu Yunusa¹ & Y. B. Usman²

¹ Department of Mathematics and Statistics, Federal Polytechnic Nasarawa, Nasarawa State, Nigeria

² Department of Mathematics and Statistics, Federal Polytechnic Idah, Kogi State, Nigeria

* Correspondence: ganakamusak@gmail.com

Abstract: Classical lifetime models such as the Half Logistic (HL) and Weibull distributions, though widely applied in reliability and survival analysis, often exhibit limitations in capturing complex data structures such as heavy tails, multimodality, or non-monotonic hazard rate patterns. To overcome these shortcomings, this study proposes a novel and more flexible model called the Odd Weibull – Half Logistic (OW-HL) distribution. By integrating the Weibull generator with the Half Logistic baseline, the OW-HL distribution extends the modeling capability of its predecessors, providing a wide range of shapes for its probability density and hazard functions, including increasing, decreasing, bathtub, and unimodal forms. Several theoretical properties of the proposed model are derived, including moments, quantile function, entropy measures, and order statistics. Parameter estimation was performed using the maximum likelihood approach, and the efficiency of the estimators was evaluated via a comprehensive Monte Carlo simulation assessing bias, mean square error, confidence interval length, and coverage probability. Applications to three real datasets spanning materials strength and energy consumption data revealed that the OW-HL distribution consistently provides superior goodness-of-fit compared to existing competitors such as Weibull, Exponentiated Weibull, Log-Logistic, and Lomax distributions. The results confirmed the model's robustness, flexibility, and practical utility for modeling asymmetric and heavy-tailed data in applied sciences.

Keywords: entropy; half logistic distribution; lifetime data; maximum likelihood estimation; odd Weibull-half logistic distribution; order statistics; reliability analysis; simulation study; Weibull family.

Received: 8 October 2025; Revised: 27 Nov. 2025; Accepted: 3 December 2025; Published: 2 February 2026



Copyright: ©2026 the Author(s). Published by JSSCI. This is an open-access article distributed under the terms of the Creative Commons Attribution 4.0 International License (CC BY 4.0).

Journal Abbreviation: J. Stat. Sci. Comput. Intell.

1. Introduction

In statistical modeling and applied probability, lifetime distributions such as the exponential, Weibull, gamma, and logistic distributions are fundamental tools for analyzing time-to-event data across various fields, including reliability engineering, medical sciences, and actuarial research [1, 2]. Despite their widespread use and mathematical tractability, these classical models often lack the flexibility to adequately capture complex

data behaviors such as heavy tails, high skewness, and non-monotonic hazard rates commonly encountered in real-world applications [3].

Among various baseline models, the half-logistic (HL) distribution has gained significant attention in reliability and survival analysis due to its simplicity and closed-form expressions for its distribution functions [4]. The HL distribution has been successfully applied in diverse areas including biological sciences, reliability engineering, and actuarial studies [5, 6]. However, its limitations in modeling heavy-tailed data and accommodating diverse hazard rate patterns restrict its applicability in more complex practical scenarios [3, 7]. To address these limitations, numerous researchers have proposed generalizations of the HL distribution. Notable extensions include the exponential HL additive model [8], exponentiated HL family of distribution [9], power transformation of HL distribution [10], Type II HL family of distribution [11], extended HL distribution [12], transmuted HL distribution [13], HL inverse Rayleigh distribution [14], type-I generalized HL distribution [15], Type II exponentiated HL-Gompertz Topp-Leone-G family of distribution [16], HL truncated exponential distribution [17], generalized HL distribution using linear regression model [18], discrete HL distributions [19], HL generalized Rayleigh distribution [20], Marshall-Olkin-exponentiated HL-G family [21], inverted exponentiated HL distribution [22], type I HL Topp-Leone inverse Lomax distribution [23], type II exponentiated HL-Gompertz-G power series class of distribution [24], Transmuted unit exponentiated HL distribution [25], New HL distribution [26], HL exponentiated inverse Rayleigh distribution [27], Odd Beta Prime HL distribution [28], the sine power HL distribution [29] and Sine Unit exponentiated HL distribution [30].

A prominent approach for developing flexible extensions involves the use of generator techniques, commonly known as T-X families, which introduce additional shape parameters through functional transformations of baseline cumulative distribution functions [31, 32]. This methodology has proven highly effective in creating new distributions with enhanced adaptability to complex data patterns. Well-established generator families of distribution include the beta-generated [33], Kumaraswamy-generated [34], Odd Weibull-generated [7] and Lomax-generated [9] families of distribution among others.

Building on this framework, the present study introduces the Odd Weibull–Half Logistic (OW–HL) distribution as a flexible extension of the classical Half Logistic model through the Odd Weibull–G family of distribution proposed by [7]. The OW–G generator offers an elegant mechanism for enhancing baseline distributions by introducing additional shape flexibility while preserving analytical tractability. Its parsimonious structure enables the modelling of a wide range of hazard rate behaviours including increasing, decreasing, bathtub-shaped and unimodal forms making it particularly effective for lifetime and reliability data. Motivated by these desirable properties, the OW–HL distribution is developed herein to capture complex data patterns that the conventional Half Logistic or Weibull models may fail to adequately represent.

The primary objective of this study is to develop a novel extension of the Half Logistic distribution, termed the Odd Weibull–Half Logistic distribution, within the OW–G family framework. This proposed model is developed to address the inherent limitations of the classical HL distribution by introducing additional shape flexibility, thereby enabling more accurate modelling of skewed and heavy-tailed data. Through this enhancement, the OW–HL distribution aims to provide a versatile and robust tool for applications in reliability analysis, survival studies, and other fields requiring flexible statistical modelling of lifetime data.

The specific objectives of this research are:

- i. To develop the OW-HL distribution by deriving its fundamental statistical functions, including the probability density function, cumulative distribution function, survival function, hazard function, cumulative hazard function, and quantile function.
- ii. To investigate the mathematical properties of the OW-HL distribution, including moments, measures of

skewness and kurtosis, entropy measures, and order statistics.

- iii. To estimate the model parameters using maximum likelihood estimation and evaluate estimator performance through Monte Carlo simulations.
- iv. To demonstrate the practical utility of the OW-HL distribution by applying it to real-world datasets and comparing its performance against established competing models using standard goodness-of-fit criteria.

The remainder of this paper is organized as follows: Section 2 presents the methodology, including the Odd Weibull-G family of distribution and the Half-logistic distribution. Section 3 presents the mathematical formulation of the OW-HL distribution, statistical properties, and parameter estimation via maximum likelihood (theoretical results). Section 4 presents the simulation study. Section 5 demonstrates applications to real-life data, and Section 6 provides concluding remarks and future research directions.

2. Methodology

2.1. Odd Weibull G-Family of Distribution

For the baseline distribution with CDF $M(x; \xi)$ and PDF $m(x; \xi)$, the Odd Weibull-G family [7] is defined by:

$$F_{OW-G}(x; \lambda, \xi) = 1 - \exp\left\{-\lambda \left[\frac{M(x; \xi)}{1-M(x; \xi)}\right]^\beta\right\}; x > 0, \lambda, \beta > 0, \xi > 0 \quad (1)$$

$$f_{OW-G}(x; \lambda, \xi) = \frac{\lambda \beta m(x; \xi) M(x; \xi)^{\beta-1}}{(1-M(x; \xi))^{\beta+1}} \exp\left\{-\lambda \left[\frac{M(x; \xi)}{1-M(x; \xi)}\right]^\beta\right\} \quad (2)$$

where $\lambda > 0$ and $\beta > 0$ is the scale and shape parameters, $m(x; \xi)$ and $M(x; \xi)$ are the pdf and CDF of the baseline distribution and ξ is the parameter vector of the baseline distribution.

2.2. Half-Logistic Distribution

The CDF and PDF of the Half logistic distribution is given by:

$$M(x) = \frac{1-e^{-x}}{1+e^{-x}}; x > 0 \quad (3)$$

$$m(x) = \frac{2e^{-x}}{(1+e^{-x})^2}; x > 0 \quad (4)$$

3. Theoretical Results

3.1. Proposed Distribution

The CDF and the pdf of the proposed Odd Weibull (OW-HL) distribution was obtained by inserting equation (3) and (4) in equation (1) and (2) respectively. Using equation (3) and (4), we have

$$\frac{M(x; \xi)}{1-M(x; \xi)} = \frac{\frac{1-e^{-x}}{1+e^{-x}}}{1-\frac{1-e^{-x}}{1+e^{-x}}} = \frac{e^x-1}{2} \quad (5)$$

Also note the algebraic identity:

$$1 - e^{-x} = \frac{e^x-1}{e^x}, \text{ so } (1 - e^{-x})^{\beta-1} = \frac{(e^x-1)^{\beta-1}}{e^{x(\beta-1)}} \quad (6)$$

$$(1 - M(x; \xi))^{\beta+1} = \left(\frac{2e^{-x}}{1+e^{-x}}\right)^{\beta+1} \quad (7)$$

To obtain the CDF of the OW-HL distribution, substituting (5) in (1), we have:

$$F_{OW-HL}(x; \lambda, \beta) = 1 - \exp\left\{-\lambda \left[\frac{e^x-1}{2}\right]^\beta\right\}; x > 0, \lambda, \beta > 0 \tag{8}$$

To obtain the PDF of the OW-HL distribution, substitute equation (3), (4) and (6) in equation (2)

$$f_{OW-G}(x; \lambda, \beta) = \frac{\lambda\beta\left(\frac{2e^{-x}}{(1+e^{-x})^2}\right)\left(\frac{1-e^{-x}}{1+e^{-x}}\right)^{\beta-1}}{\left(\frac{2e^{-x}}{1+e^{-x}}\right)^{\beta+1}} \exp\left\{-\lambda \left[\frac{e^x-1}{2}\right]^\beta\right\} \tag{9}$$

This simplifies to:

$$f_{OW-HL}(x; \lambda, \beta) = \frac{\lambda\beta}{2^\beta} e^x (e^x - 1)^{\beta-1} \exp\left\{-\lambda \left[\frac{e^x-1}{2}\right]^\beta\right\} \tag{10}$$

where $x > 0, \lambda > 0$ and $\beta > 0$ is the scale and shape parameters of the OW-HL Distribution.

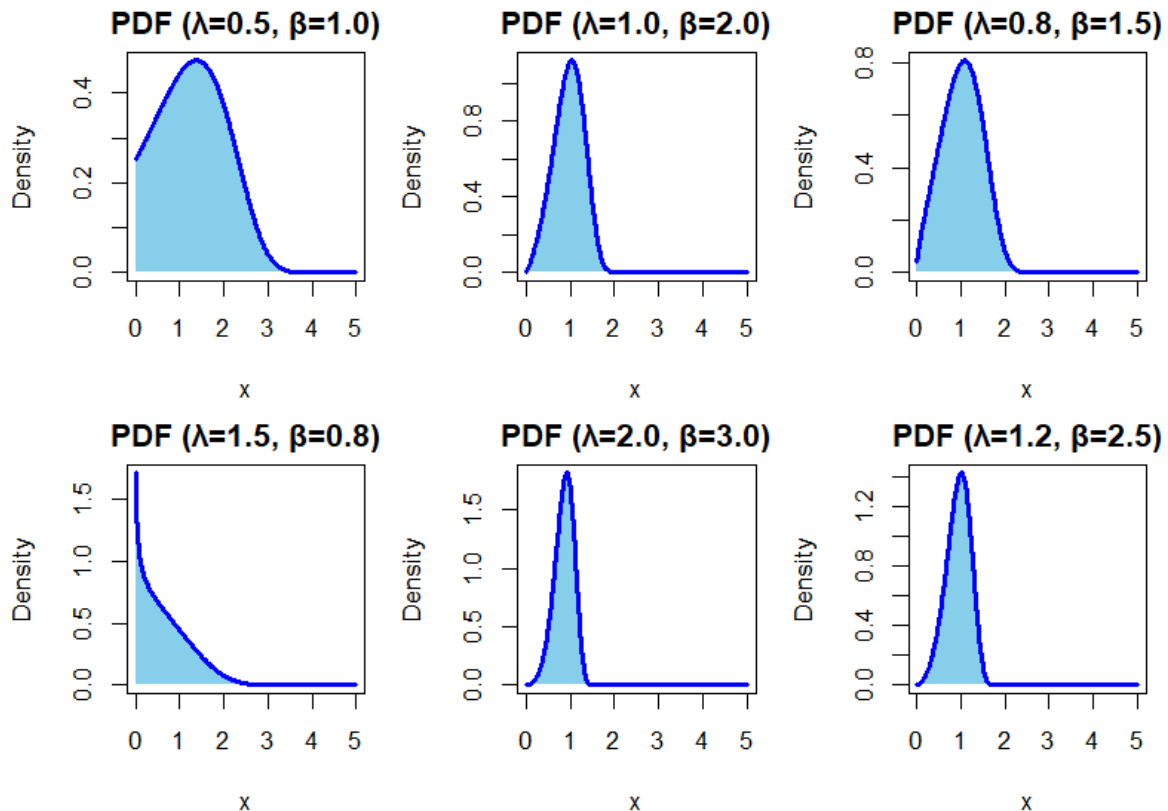


Figure 1: Plots of the PDF of the OW-HL distribution for various parameter values

Figure 1 illustrates that the OW-HL distribution exhibited a wide range of shapes, including right-skewed, symmetric and decreasing patterns, depending on the parameter values. Specifically, smaller values of λ and β yield more dispersed and flatter densities, while larger values result in sharper peaks and lighter tails. This flexibility highlights the ability of the OW-HL distribution to model diverse data behaviors encountered in reliability and lifetime data modelling.

Figure 2 presents the CDF plots of the OW-HL distribution for various parameter combinations of λ and β . The CDF curves demonstrated that the distribution is continuous and strictly increasing, confirming its suitability for modeling positive-valued data. As the parameters λ and β increase, the curves approach unity more rapidly, indicating faster accumulation of probability mass and lighter tails. Conversely, smaller parameter values produce more gradual curves, representing heavier-tailed behavior. These results highlight the OW-HL distribution’s flexibility in capturing a wide spectrum of cumulative probability structures encountered in lifetime and reliability data modeling.

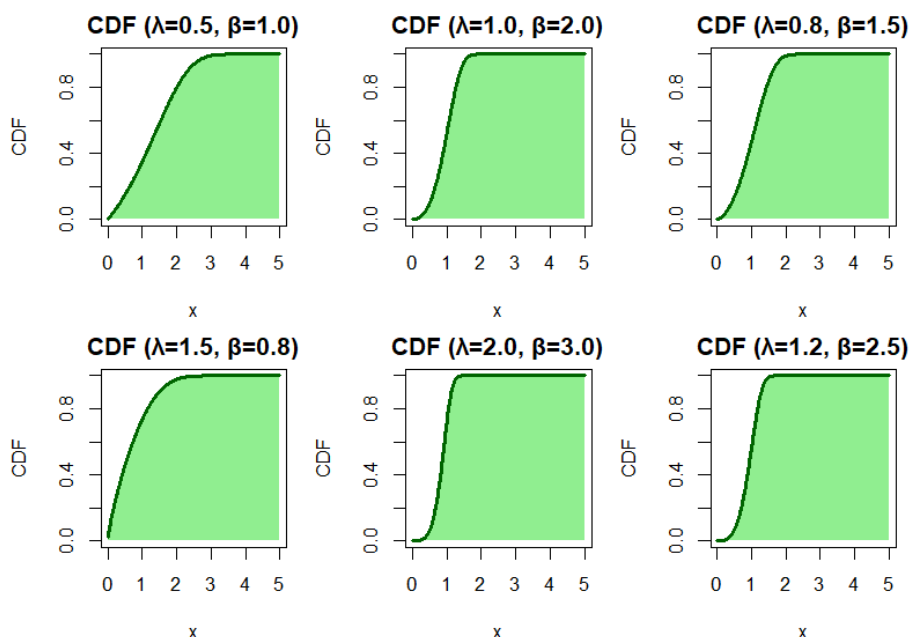


Figure 2: Plots of the CDF of the OW-HL distribution for various parameter values

3.2. Mathematical Properties of OW-HL Distribution

3.2.1. The Survival Function

The survival function $S(x)$ of OW-HL distribution given by:

$$S(x) = 1 - F_{OW-HL}(x; \lambda, \beta); \quad x > 0, \lambda > 0 \text{ and } \beta > 0 \quad (11)$$

where $F_{OW-HL}(x; \lambda, \beta)$ is the CDF of the OW-HL distribution. Substituting (8) in (11) yielded the survival function of OW-HL distribution as:

$$S(x) = \exp \left\{ -\lambda \left[\frac{e^x - 1}{2} \right]^\beta \right\}; \quad x > 0, \lambda, \beta > 0 \quad (12)$$

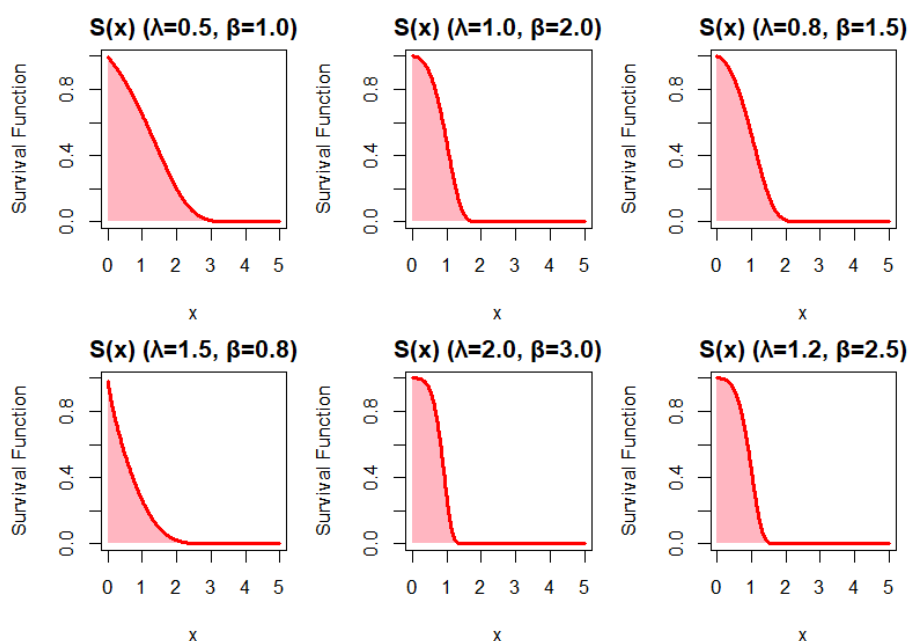


Figure 3: Plots of the survival function of the OW-HL distribution for various parameter values

Figure 3 displayed the survival function of the OW–HL distribution for different combinations of the parameters λ and β . As expected, all survival curves exhibit a monotonically decreasing pattern, indicating a decline in survival probability with increasing x . Larger values of λ and β resulted in a steeper decay of the survival function, signifying shorter lifetimes or higher failure rates, whereas smaller values of the parameters correspond to slower decay and longer survival times. These patterns demonstrate the flexibility of the OW–HL distribution in capturing various survival behaviors, ranging from rapid to gradual failure processes commonly observed in lifetime and reliability studies.

3.2.2. The Hazard Function

The hazard function $h(x)$ of a distribution is obtain using the relation $h(x) = \frac{f(x)}{S(x)}$, [1, 35] where $f(x)$ and $S(x)$ is the PDF and survival function respectively of the given distribution. Thus, the hazard of OW-HL distribution is given as:

$$\begin{aligned}
 h(x) = \frac{f(x)}{S(x)} &= \frac{\frac{\lambda\beta}{2^\beta} e^x ((e^x - 1))^{\beta-1} \exp\left\{-\lambda \left[\frac{e^x - 1}{2}\right]^\beta\right\}}{\exp\left\{-\lambda \left[\frac{e^x - 1}{2}\right]^\beta\right\}} \\
 &= \frac{\lambda\beta}{2^\beta} e^x ((e^x - 1))^{\beta-1}
 \end{aligned}
 \tag{13}$$

The hazard function plots of the OW–HL distribution in figure 4 displayed a consistently increasing trend across all parameter combinations, indicating a positive aging or wear-out behaviour. The scale parameter (λ) governs the overall magnitude of the hazard rate, whereas the shape parameter (β) controls the curvature and steepness of its rise. Higher values of β produce sharper and more rapidly increasing hazards, aligning with the right-skewed patterns observed in the PDF and quantile plots. These results demonstrate the OW–HL distribution’s flexibility in modeling lifetime data characterized by accelerating failure rates and varying intensities of aging.

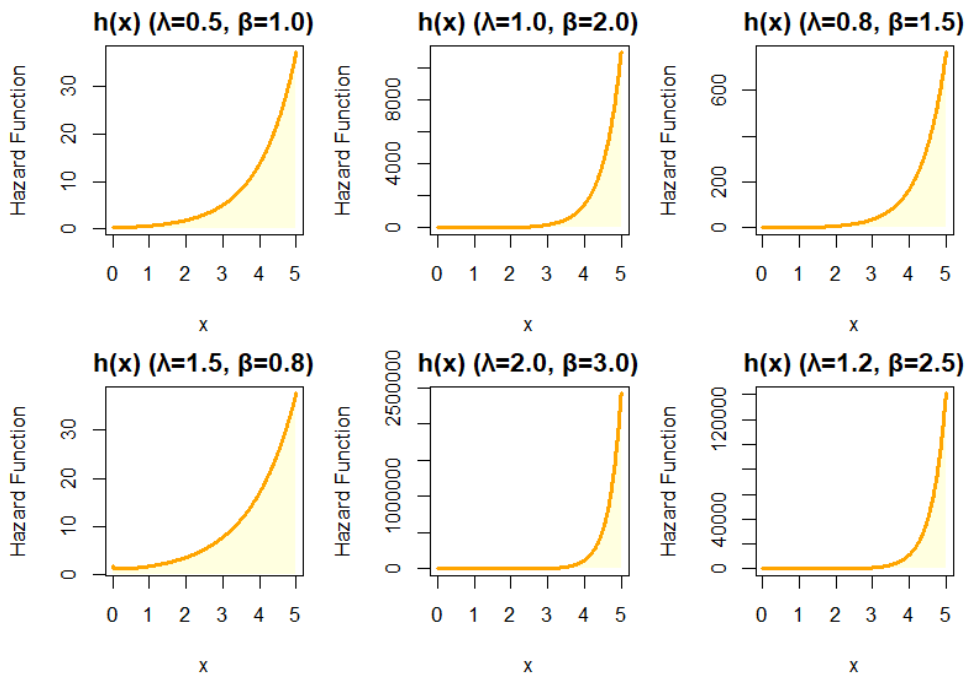


Figure 4: Plots of the hazard function of the OW-HL distribution for various parameter values

3.2.3. The Cumulative Hazard Function

Given the survival function of distribution, the cumulative hazard function $H(x)$ of a distribution is obtain using the relation $H(x) = -\ln[S(x)]$ [36, 37]. Thus, the cumulative hazard function of OW-HL distribution was obtained using the relation:

$$\begin{aligned}
 H(x) &= -\ln\left(\exp\left\{-\lambda\left[\frac{e^x-1}{2}\right]^\beta\right\}\right) \\
 &= \lambda\left[\frac{e^x-1}{2}\right]^\beta
 \end{aligned}
 \tag{14}$$

Table 1: Numerical Values of Distribution Functions for the OW-HL Distribution for various parameter values (λ and β) combinations.

X	λ	β	PDF	CDF	Survival	Hazard	CumHazard
0.5	0.5	1.0	0.3505	0.1497	0.8503	0.4122	0.1622
1.0	0.5	1.0	0.4423	0.3492	0.6508	0.6796	0.4296
1.5	0.5	1.0	0.4692	0.5812	0.4188	1.1204	0.8704
2.0	0.5	1.0	0.3740	0.7976	0.2025	1.8473	1.5973
2.5	0.5	1.0	0.1860	0.9389	0.0611	3.0456	2.7956
3.0	0.5	1.0	0.0425	0.9915	0.0085	5.0214	4.7714
0.5	1.0	2.0	0.4814	0.0999	0.9001	0.5348	0.1052
1.0	1.0	2.0	1.1163	0.5220	0.4780	2.3354	0.7381
1.5	1.0	2.0	0.3768	0.9517	0.0483	7.8019	3.0305
2.0	1.0	2.0	0.0009	1.0000	0.0000	23.6045	10.2050
2.5	1.0	2.0	0.0000	1.0000	0.0000	68.1153	31.2620
3.0	1.0	2.0	0.0000	1.0000	0.0000	191.6716	91.0644
0.5	0.8	1.5	0.4860	0.1374	0.8626	0.5634	0.1478
1.0	0.8	1.5	0.7995	0.4712	0.5288	1.5117	0.6371
1.5	0.8	1.5	0.5649	0.8408	0.1592	3.5479	1.8375
2.0	0.8	1.5	0.0823	0.9896	0.0104	7.9240	4.5677
2.5	0.8	1.5	0.0004	1.0000	0.0000	17.2839	10.5768
3.0	0.8	1.5	0.0000	1.0000	0.0000	37.2282	23.5831
0.5	1.5	0.8	0.6736	0.4563	0.5437	1.2391	0.6094
1.0	1.5	0.8	0.4453	0.7351	0.2649	1.6813	1.3284
1.5	1.5	0.8	0.2325	0.9034	0.0966	2.4068	2.3372
2.0	1.5	0.8	0.0787	0.9776	0.0224	3.5145	3.7985
2.5	1.5	0.8	0.0136	0.9974	0.0026	5.1807	5.9443
3.0	1.5	0.8	0.0008	0.9999	0.0001	7.6754	9.1166
0.5	1.2	2.5	0.4252	0.0694	0.9306	0.4569	0.0719
1.0	1.2	2.5	1.4287	0.5600	0.4400	3.2470	0.8210
1.5	1.2	2.5	0.1273	0.9918	0.0082	15.4409	4.7982
2.0	1.2	2.5	0.0000	1.0000	0.0000	63.2835	21.8876
2.5	1.2	2.5	0.0000	1.0000	0.0000	241.5964	88.7060
3.0	1.2	2.5	0.0000	1.0000	0.0000	888.1499	337.5726
0.5	2.0	3.0	0.4861	0.0660	0.9340	0.5204	0.0683

1.0	2.0	3.0	1.6933	0.7187	0.2813	6.0193	1.2683
1.5	2.0	3.0	0.0011	1.0000	0.0000	40.7458	10.5514
2.0	2.0	3.0	0.0000	1.0000	0.0000	226.2162	65.2004
2.5	2.0	3.0	0.0000	1.0000	0.0000	1142.5489	349.5876
3.0	2.0	3.0	0.0000	1.0000	0.0000	5487.2339	1738.0135

Table 1 displays numerical values of the PDF, CDF, survival, hazard, and cumulative hazard functions of the OW-HL distribution for various parameter combinations. The results showed that increasing λ and β sharpens the PDF peak and accelerates the decay of the survival function. Correspondingly, the hazard and cumulative hazard values rise rapidly with xxx, illustrating the distribution’s flexibility in capturing diverse lifetime behaviors ranging from light- to heavy-tailed patterns.

3.2.4. Quantile Function

The quantile function $Q(u)$, is obtain by inverting the CDF [38]. Specifically, for a given probability $u \in (0,1)$, $Q(u)$ is obtained by solving

$$F_{OW-HL}(x) = u \tag{15}$$

$$1 - \exp \left\{ -\lambda \left[\frac{e^x - 1}{2} \right]^\beta \right\} = u$$

$$x = \ln \left(1 + 2 \left[-\frac{1}{\lambda} \ln (1 - u) \right]^{\frac{1}{\beta}} \right)$$

Thus, the quantile function of OW-HL distribution is given by:

$$Q_{OW-HL}(u; \lambda, \beta) = \ln \left(1 + 2 \left[-\frac{1}{\lambda} \ln (1 - u) \right]^{\frac{1}{\beta}} \right), 0 \leq u < 1, \lambda > 0, \beta > 0 \tag{16}$$

Table 2: Numerical values of the quantiles Function of OW-HL distribution for different parameter (λ, β) combinations

u	(λ, β)					
	(0.5, 1.0)	(1.0, 2.0)	(0.8, 1.5)	(1.5, 0.8)	(1.2, 2.5)	(2.0, 3.0)
0.1	0.3517	0.5003	0.4172	0.0690	0.5629	0.5595
0.2	0.6379	0.6651	0.6172	0.1696	0.7033	0.6743
0.3	0.8865	0.7859	0.7734	0.2868	0.8025	0.7541
0.4	1.1129	0.8877	0.9094	0.4189	0.8843	0.8193
0.5	1.3278	0.9802	1.0359	0.5664	0.9577	0.8775
0.6	1.5402	1.0697	1.1598	0.7324	1.0280	0.9329
0.7	1.7606	1.1614	1.2883	0.9240	1.0995	0.9891
0.8	2.0066	1.2624	1.4321	1.1581	1.1784	1.0509
0.9	2.3234	1.3950	1.6188	1.4855	1.2797	1.1302

Table 2 presents the quantile values of the OW-HL distribution under various combinations of the parameters λ and β . As the quantile level u increases, the corresponding quantile values also rise, reflecting the typical right-skewed behavior of the distribution for the selected parameter sets. Higher values of λ and β tend to compress the distribution toward smaller quantile values, demonstrating the sensitivity of the OW-HL model to parameter variation and its adaptability across different data scales. Although the reported results

exhibit a predominantly right-skewed pattern, the OW-HL distribution remains highly flexible; by appropriately adjusting the shape parameter β and the scale parameter λ , it can effectively model symmetric, left-skewed, and bathtub-shaped patterns in both density and hazard structures.

3.2.5. The Raw Moments

According to [39], the r^{th} raw moment about the origin is defined as:

$$\mu'_r = E[X^r] = \int_0^\infty x^r f_{OW-HL}(x; \lambda, \beta) dx \quad (17)$$

where $f_{OW-HL}(x; \lambda, \beta)$ is the PDF of the OW-HL distribution. Thus, given the PDF of OW-HL distribution, the r^{th} is derived as follows:

$$\mu'_r = E[X^r] = \int_0^\infty x^r \frac{\lambda \beta}{2^\beta} e^x (e^x - 1)^{\beta-1} \exp\left\{-\lambda \left[\frac{e^x-1}{2}\right]^\beta\right\} dx$$

By applying the transformation,

$$y = \frac{e^x-1}{2} \Rightarrow x = \ln(1 + 2y), dx = \frac{2}{1+2y} dy, \text{ the moment integral simplifies to}$$

$$\mu'_r = \lambda \beta \int_0^\infty [\ln(1 + 2y)]^r y^{\beta-1} e^{-\lambda y^\beta} dy$$

with the substitution $t = y^\beta$, this reduces to

$$\mu'_r = \lambda \int_0^\infty \left[\ln\left(1 + 2t^{1/\beta}\right)\right]^r e^{-\lambda t} dt \quad (18)$$

Equivalently, if $T \sim \text{Exp}(\lambda)$, then

$$\mu'_r = E\left[\left(\ln\left(1 + 2T^{1/\beta}\right)\right)^r\right] \quad (19)$$

3.2.6. The Mean and Variance

The mean and variance of OW-HL distribution from the raw moment in equation (18) or its equivalent in (19) for $r = 1, 2$ are given by:

i. **The mean**

$$\mu = \mu'_1 = E(X) = \lambda \int_0^\infty \ln\left(1 + 2t^{1/\beta}\right) e^{-\lambda t} dt = E\left[\ln\left(1 + 2T^{1/\beta}\right)\right], T \sim \text{Exp}(\lambda) \quad (20)$$

ii. **The variance**

$$\sigma^2 = \mu'_2 - (\mu'_1)^2$$

$$\text{where } \mu'_2 = \lambda \int_0^\infty \left[\ln\left(1 + 2t^{1/\beta}\right)\right]^2 e^{-\lambda t} dt = E\left[\left(\ln\left(1 + 2T^{1/\beta}\right)\right)^2\right], T \sim \text{Exp}(\lambda) \quad (21)$$

Figure 5 illustrates the 3D surface plots of the mean and variance of the OW-HL distribution as functions of the shape parameter (β) and scale parameter (λ). The mean surface shows a smooth, gradual increase as β and λ vary, indicating sensitivity of the central tendency to parameter changes. In contrast, the variance surface remains relatively low and stable across most parameter combinations, reflecting limited dispersion. Both plots demonstrate that while the OW-HL distribution's location shifts with parameter variations, its spread remains moderately constrained, highlighting its stability and adaptability for modelling diverse data patterns.

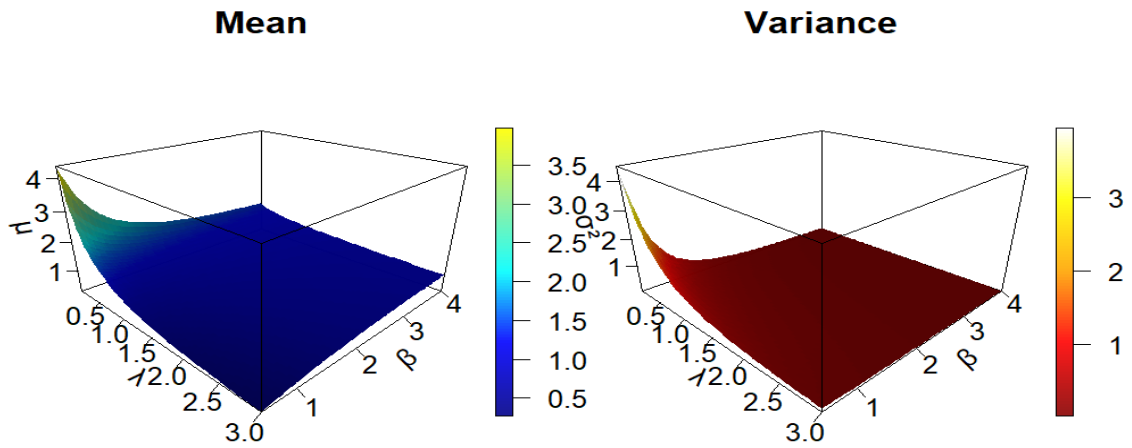


Figure 5: 3D plots of mean and variance of OW-HL distribution

3.2.7. Skewness and Kurtosis

The skewness γ_1 and kurtosis γ_2 are respectively given by:

$$\gamma_1 = \frac{\mu'_3 - 3\mu\sigma^2 - \mu^3}{\sigma^3} \quad (22)$$

and

$$\gamma_2 = \frac{\mu'_4}{\sigma^4} \quad (23)$$

where $\mu'_3 = \lambda \int_0^\infty [\ln(1 + 2t^{1/\beta})]^3 e^{-\lambda t} dt = E\left[\left(\ln(1 + 2T^{1/\beta})\right)^3\right], T \sim \text{Exp}(\lambda)$ and

$\mu'_4 = \lambda \int_0^\infty [\ln(1 + 2t^{1/\beta})]^4 e^{-\lambda t} dt = E\left[\left(\ln(1 + 2T^{1/\beta})\right)^4\right], T \sim \text{Exp}(\lambda)$

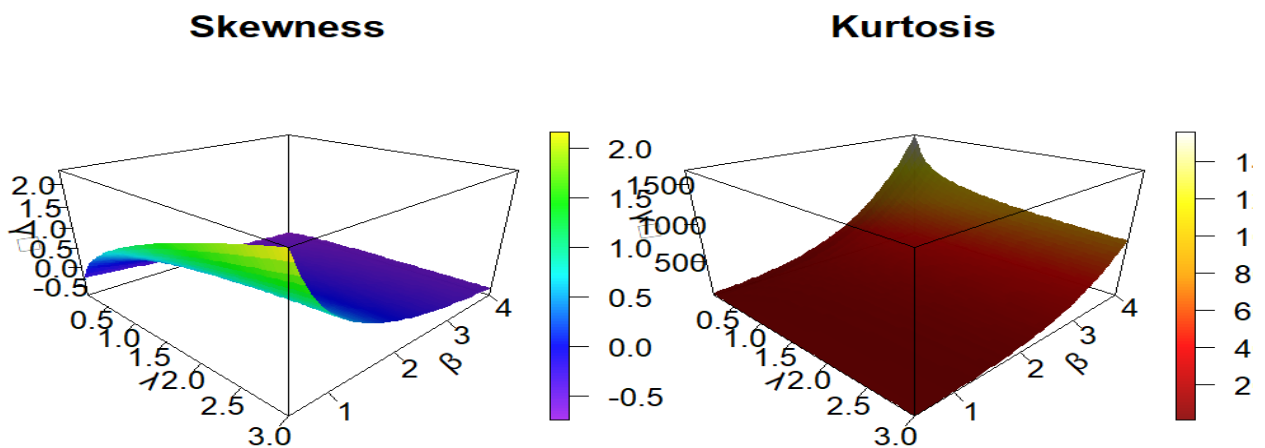


Figure 6: 3D plots of skewness and kurtosis of OW-HL distribution

Figure 6 presents the 3D surface plots of the skewness (γ_1) and kurtosis (γ_2) of the OW-HL distribution as functions of the shape parameter (β) and scale parameter (λ). The skewness surface shows a smooth transition from negative to positive values, indicating that the distribution can capture left-skewed, symmetric, and right-skewed behaviors depending on parameter combinations. The kurtosis surface, on the other hand, exhibited a

sharp rise in certain parameter regions, with values increasing rapidly as β and λ vary, reflecting the potential for heavy-tailed or leptokurtic characteristics. Together, these plots highlighted the high flexibility of the OW-HL distribution in modeling data with diverse asymmetry and tail behavior.

Table 3: Numerical values of the Moments of OW-HL Distribution for various parameter values (λ and β) combinations.

X	λ	β	Mean	Variance	Skewness	Kurtosis
0.5	0.5	1.0	1.3409	0.5320	0.1685	35.2301
1.0	0.5	1.0	1.3409	0.5320	0.1685	35.2301
1.5	0.5	1.0	1.3409	0.5320	0.1685	35.2301
2.0	0.5	1.0	1.3409	0.5320	0.1685	35.2301
2.5	0.5	1.0	1.3409	0.5320	0.1685	35.2301
3.0	0.5	1.0	1.3409	0.5320	0.1685	35.2301
0.5	1.0	2.0	0.9636	0.1150	-0.1695	114.3245
1.0	1.0	2.0	0.9636	0.1150	-0.1695	114.3245
1.5	1.0	2.0	0.9636	0.1150	-0.1695	114.3245
2.0	1.0	2.0	0.9636	0.1150	-0.1695	114.3245
2.5	1.0	2.0	0.9636	0.1150	-0.1695	114.3245
3.0	1.0	2.0	0.9636	0.1150	-0.1695	114.3245
0.5	0.8	1.5	1.0294	0.2023	0.0141	61.4318
1.0	0.8	1.5	1.0294	0.2023	0.0141	61.4318
1.5	0.8	1.5	1.0294	0.2023	0.0141	61.4318
2.0	0.8	1.5	1.0294	0.2023	0.0141	61.4318
2.5	0.8	1.5	1.0294	0.2023	0.0141	61.4318
3.0	0.8	1.5	1.0294	0.2023	0.0141	61.4318
0.5	1.5	0.8	0.6856	0.3029	0.8637	19.2089
1.0	1.5	0.8	0.6856	0.3029	0.8637	19.2089
1.5	1.5	0.8	0.6856	0.3029	0.8637	19.2089
2.0	1.5	0.8	0.6856	0.3029	0.8637	19.2089
2.5	1.5	0.8	0.6856	0.3029	0.8637	19.2089
3.0	1.5	0.8	0.6856	0.3029	0.8637	19.2089
0.5	1.2	2.5	0.9378	0.0755	-0.3118	204.0125
1.0	1.2	2.5	0.9378	0.0755	-0.3118	204.0125
1.5	1.2	2.5	0.9378	0.0755	-0.3118	204.0125
2.0	1.2	2.5	0.9378	0.0755	-0.3118	204.0125
2.5	1.2	2.5	0.9378	0.0755	-0.3118	204.0125
3.0	1.2	2.5	0.9378	0.0755	-0.3118	204.0125
0.5	2.0	3.0	0.8591	0.0486	-0.3902	318.3138
1.0	2.0	3.0	0.8591	0.0486	-0.3902	318.3138
1.5	2.0	3.0	0.8591	0.0486	-0.3902	318.3138
2.0	2.0	3.0	0.8591	0.0486	-0.3902	318.3138
2.5	2.0	3.0	0.8591	0.0486	-0.3902	318.3138
3.0	2.0	3.0	0.8591	0.0486	-0.3902	318.3138

Table 3 summarizes the numerical values of the mean, variance, skewness, and kurtosis of the OW-HL distribution for different combinations of the parameters λ and β . The results showed that as λ and β vary, both the mean and variance change noticeably, reflecting the strong influence of these parameters on the distribution's scale and spread. The skewness values alternate between positive and negative, confirming the OW-HL distribution's ability to capture both right- and left-skewed data. Moreover, the high kurtosis values across all settings indicate heavy-tailed behavior, suggesting that the OW-HL model can effectively describe data with significant tail variation or extreme observations.

3.2.8. Entropy Measures

a) Renyi Entropy

For a continuous random variable X with PDF $f(x)$, the Renyi entropy of order $K > 0, K \neq 1$ is defined as:

$$H_K = \frac{1}{1-K} \log \left(\int_0^{\infty} [f_{OW-HL}(x; \lambda, \beta)]^K dx \right) \quad (24)$$

where $f_{OW-HL}(x; \lambda, \beta)$ is the PDF of OW-HL distribution given in (10). We therefore need to evaluate:

$I_K = \int_0^{\infty} [f_{OW-HL}(x; \lambda, \beta)]^K dx$ and then $H_K = \frac{1}{1-K} \log(I_K)$. Raising the PDF to power K , yielded;

$$[f_{OW-HL}(x; \lambda, \beta)]^K = \left(\frac{\lambda\beta}{2\beta}\right)^K e^{Kx} (e^x - 1)^{K(\beta-1)} \exp \left\{ -K\lambda \left[\frac{e^x - 1}{2} \right]^\beta \right\}$$

Hence,

$$I_K = \left(\frac{\lambda\beta}{2\beta}\right)^K \int_0^{\infty} e^{Kx} (e^x - 1)^{K(\beta-1)} \exp \left\{ -K\lambda \left[\frac{e^x - 1}{2} \right]^\beta \right\} dx$$

Let $y = \frac{e^x - 1}{2} \Rightarrow x = \ln(1 + 2y), dx = \frac{2}{1+2y} dy$, with $y \in (0, \infty)$ as x runs from 0 to ∞ . Under this change,

$e^{Kx} = (1 + 2y)^K$; $(e^x - 1)^{K(\beta-1)} = (2y)^{K(\beta-1)}$; $\exp \left\{ -K\lambda \left[\frac{e^x - 1}{2} \right]^\beta \right\} = e^{-K\lambda y^\beta}$. Thus, substituting in I_K gives:

$$I_K = \left(\frac{\lambda\beta}{2\beta}\right)^K \int_0^{\infty} (1 + 2y)^K (2y)^{K(\beta-1)} e^{-K\lambda y^\beta} \frac{2}{1+2y} dy$$

$$I_K = (\lambda\beta)^K 2^{1-K} \int_0^{\infty} y^{K(\beta-1)} (1 + 2y)^{K-1} e^{-K\lambda y^\beta} dy$$

Thus, the Renyi entropy then follows as:

$$H_K = \frac{1}{1-K} \log \left\{ (\lambda\beta)^K 2^{1-K} \int_0^{\infty} y^{K(\beta-1)} (1 + 2y)^{K-1} e^{-K\lambda y^\beta} dy \right\} \quad (25)$$

Tsallis Entropy

For a continuous random variable X with PDF $f(x)$, the Tsallis entropy of order $K > 0, K \neq 1$ is defined as:

$$T_K(X) = \frac{1}{K-1} \left(1 - \int_0^{\infty} [f_{OW-HL}(x; \lambda, \beta)]^K dx \right) \quad (26)$$

Let $I_K = \int_0^{\infty} [f_{OW-HL}(x; \lambda, \beta)]^K dx$ where $f_{OW-HL}(x; \lambda, \beta)$ is the PDF of the OW-HL distribution defined in (10). We have already derived the:

$$I_K = (\lambda\beta)^K 2^{1-K} \int_0^{\infty} y^{K(\beta-1)} (1 + 2y)^{K-1} e^{-K\lambda y^\beta} dy$$

Thus, the Tsallis entropy for the OW-HL distribution of order K is given by:

$$T_K(X) = \frac{1}{K-1} \left(1 - (\lambda\beta)^K 2^{1-K} \int_0^{\infty} y^{K(\beta-1)} (1 + 2y)^{K-1} e^{-K\lambda y^\beta} dy \right) \quad (27)$$

Table 4: Numerical results of Rényi and Tsallis entropies for the OW-HL distribution

λ	β	Rényi Entropy			Tsallis Entropy		
		$K = 0.5$	$K = 1.5$	$K = 2.5$	$K = 0.5$	$K = 1.5$	$K = 2.5$
0.5	0.8	1.2843	1.1588	1.1107	1.8011	0.8795	0.5407
0.5	1.0	1.1223	1.0064	0.9620	1.5055	0.7908	0.5092
0.5	1.5	0.8139	0.6534	0.5804	1.0045	0.5574	0.3875
0.5	2.0	0.5816	0.3770	0.2895	0.6750	0.3436	0.2348
0.5	2.5	0.3933	0.1563	0.0609	0.4346	0.1504	0.0582
0.5	3.0	0.2344	-0.0261	-0.1264	0.2487	-0.0262	-0.1392
0.8	0.8	1.0887	0.9117	0.8276	1.4469	0.7322	0.4740
0.8	1.0	0.9571	0.8253	0.7797	1.2275	0.6762	0.4597
0.8	1.5	0.6973	0.5431	0.4749	0.8343	0.4756	0.3397
0.8	2.0	0.4929	0.2968	0.2126	0.5590	0.2758	0.1821
0.8	2.5	0.3224	0.0930	-0.0001	0.3498	0.0909	-0.0001
0.8	3.0	0.1756	-0.0785	-0.1772	0.1836	-0.0801	-0.2029
1.0	0.8	0.9813	0.7690	0.6587	1.2667	0.6384	0.4185
1.0	1.0	0.8679	0.7226	0.6727	1.0866	0.6065	0.4236
1.0	1.5	0.6360	0.4831	0.4167	0.7488	0.4292	0.3098
1.0	2.0	0.4471	0.2544	0.1717	0.5011	0.2389	0.1514
1.0	2.5	0.2862	0.0602	-0.0319	0.3077	0.0593	-0.0327
1.0	3.0	0.1460	-0.1053	-0.2032	0.1514	-0.1081	-0.2376
1.2	0.8	0.8860	0.6402	0.5054	1.1147	0.5479	0.3543
1.2	1.0	0.7894	0.6304	0.5752	0.9679	0.5407	0.3853
1.2	1.5	0.5831	0.4303	0.3650	0.6770	0.3871	0.2810
1.2	2.0	0.4080	0.2176	0.1361	0.4526	0.2062	0.1231
1.2	2.5	0.2555	0.0320	-0.0592	0.2725	0.0317	-0.0619
1.2	3.0	0.1209	-0.1282	-0.2254	0.1246	-0.1324	-0.2682
1.5	0.8	0.7597	0.4679	0.3010	0.9242	0.4172	0.2422
1.5	1.0	0.6865	0.5075	0.4437	0.8191	0.4482	0.3240
1.5	1.5	0.5146	0.3609	0.2966	0.5868	0.3302	0.2394
1.5	2.0	0.3578	0.1699	0.0897	0.3918	0.1629	0.0839
1.5	2.5	0.2164	-0.0042	-0.0944	0.2285	-0.0042	-0.1014
1.5	3.0	0.0890	-0.1573	-0.2538	0.0911	-0.1637	-0.3089
2.0	0.8	0.5806	0.2231	0.0144	0.6737	0.2111	0.0143
2.0	1.0	0.5421	0.3329	0.2556	0.6227	0.3066	0.2123
2.0	1.5	0.4202	0.2637	0.1999	0.4676	0.2471	0.1727
2.0	2.0	0.2894	0.1040	0.0253	0.3114	0.1014	0.0248
2.0	2.5	0.1635	-0.0537	-0.1427	0.1703	-0.0544	-0.1591
2.0	3.0	0.0463	-0.1968	-0.2924	0.0468	-0.2068	-0.3669

Table 4 presents the computed Rényi and Tsallis entropies of the OW–HL distribution for different combinations of the parameters λ , β , and entropy order K . The results revealed that both entropy measures decrease as β increases, reflecting reduced uncertainty and greater concentration of probability mass for higher shape parameters. Conversely, smaller β or λ values yield higher entropy, indicating greater

dispersion and randomness. Additionally, Rényi and Tsallis entropies exhibit consistent behavior across varying K , confirming their agreement in quantifying the distribution’s uncertainty structure and flexibility across parameter configurations.

Rényi and Tsallis entropies ($K=1.5$)

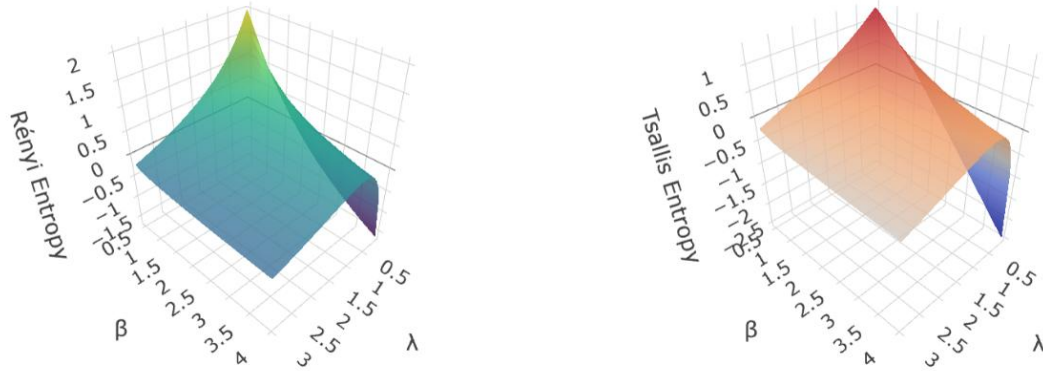


Figure 7: 3D plots of Rényi and Tsallis entropies for the OW-HL distribution ($K = 1.5$)

Figure 7 presents the three-dimensional surface plots of the Rényi and Tsallis entropies of the OW-HL distribution as functions of the scale parameter (λ) and shape parameter (β) for order ($K = 1.5$). Both entropies surfaces exhibited smooth, tent-shaped structures with distinct peak regions, indicating that the distribution’s uncertainty varies systematically with parameter combinations. The similarity in their topographies suggested that both measures capture comparable patterns of information content, confirming the OW-HL distribution’s flexibility in representing varying levels of randomness and structural complexity across different parameter settings.

Rényi and Tsallis entropies ($K=2.5$)

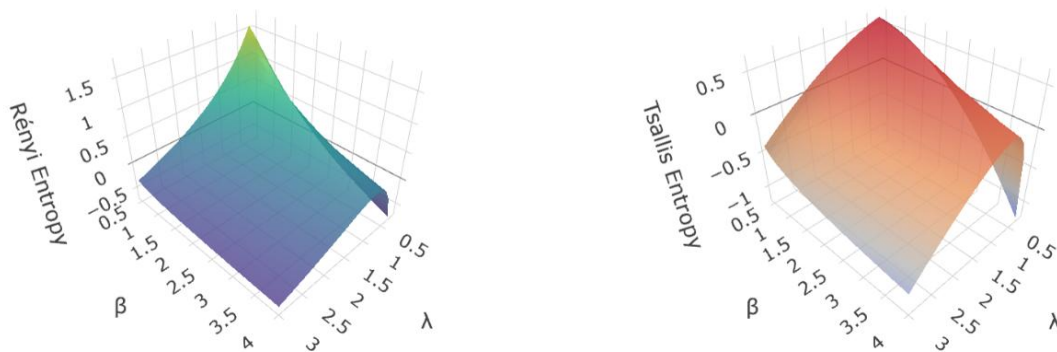


Figure 8: 3D plots of Rényi and Tsallis entropies for the OW-HL distribution ($K = 2.5$)

Figure 8 presents the three-dimensional surface plots of the Rényi and Tsallis entropies of the OW-HL distribution as functions of the scale parameter (λ) and shape parameter (β) for order ($K = 2.5$). Both entropies surfaces exhibited smooth, pyramid-like structures with systematic variation in information content across the parameter space. Compared to ($K = 1.5$) (Figure 7), the entropy ranges are slightly compressed, indicating reduced sensitivity to tail behaviour as K increases. The consistent geometric patterns across both measures reaffirmed their close theoretical relationship and demonstrated the OW-HL distribution’s flexibility in

modelling varying degrees of uncertainty and information content under different parameter configurations.

3.2.9. Order Statistics

Suppose X_1, X_2, \dots, X_n are random sample from OW-HL distribution with CDF $F(x)$ and PDF $f(x)$, the PDF of the k^{th} order statistic $Y_{(k)}$ is given by:

$$f_{X_{(k)}}(x) = \frac{n!}{(k-1)!(n-k)!} [F(x)]^{k-1} [1 - F(x)]^{n-k} f(x) \tag{28}$$

Using the relation $F(x) = 1 - S(x)$ and $S(x) = \exp\left\{-\lambda \left[\frac{e^x - 1}{2}\right]^\beta\right\}$, we get:

$[F(x)]^{k-1} = (1 - S(x))^{k-1}$, $[1 - F(x)]^{n-k} = [S(x)]^{n-k}$, substituting in equation (28), we have:

$$\begin{aligned} f_{X_{(k)}}(x) &= \frac{n!}{(k-1)!(n-k)!} (1 - S(x))^{k-1} [S(x)]^{n-k} \frac{\lambda\beta}{2^\beta} e^x (e^x - 1)^{\beta-1} S(x) \\ &= \frac{n!}{(k-1)!(n-k)!} \frac{\lambda\beta}{2^\beta} e^x (e^x - 1)^{\beta-1} (1 - S(x))^{k-1} [S(x)]^{n-k+1} \end{aligned} \tag{29}$$

Now, substituting $S(x) = \exp\left\{-\lambda \left[\frac{e^x - 1}{2}\right]^\beta\right\}$ in equation (29), we have:

$$f_{X_{(k)}}(x) = \frac{n!}{(k-1)!(n-k)!} \frac{\lambda\beta}{2^\beta} e^x (e^x - 1)^{\beta-1} \left(1 - \exp\left\{-\lambda \left[\frac{e^x - 1}{2}\right]^\beta\right\}\right)^{k-1} \left[\exp\left\{-\lambda \left[\frac{e^x - 1}{2}\right]^\beta\right\}\right]^{n-k+1} \tag{30}$$

PDFs of Order Statistics for OW-HL Distribution

$\lambda = 1, \beta = 2, n = 10$

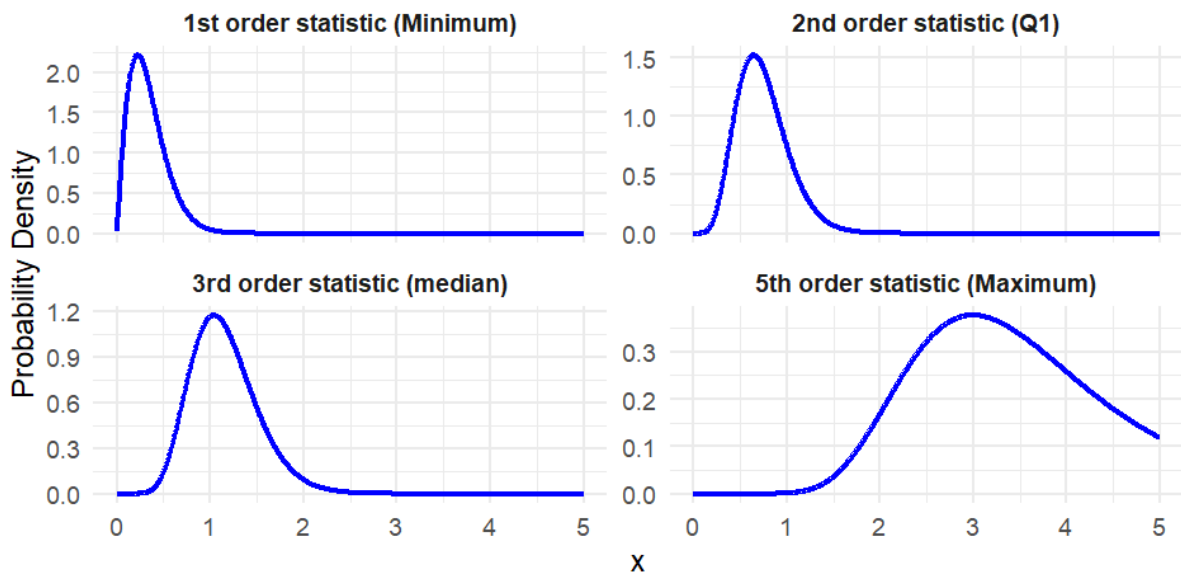


Figure 9: Plot of PDFs for order statistics of the OW-HL distribution

Figure 9 presents the probability density functions of selected order statistics from the OW-HL distribution with parameters ($\lambda = 1$) and ($\beta = 2$). The plots illustrated the 1st (minimum), 2nd (first quartile (Q_1), 3rd (median) and 5th (maximum) order statistics, each exhibited distinct shapes corresponding to their sample positions. The minimum and Q_1 statistics showed pronounced right-skewed densities concentrated near lower values, while the median displays a more symmetric, bell-shaped form. The maximum statistic revealed a wider, right-shifted distribution with lower peak density, reflecting greater variability at higher order levels. This finding demonstrated how the OW-HL distribution’s order statistics transition from sharply peaked, skewed forms at

lower orders to broader, more symmetric patterns at higher orders, highlighting its flexibility in modelling ordered data and reliability-related phenomena.

Table 5: Numerical results of the order statistics for the OW-HL distribution

λ	β	1 th Percentile	5 th Percentile	25 th Percentile	50 th Percentile	75 th Percentile	99 th Percentile	99.9 th Percentile
0.5	1.0	0.0394	0.1866	0.7658	1.3278	1.8787	2.9664	3.3545
1.0	1.0	0.0199	0.0977	0.4545	0.8697	1.3278	2.3234	2.6957
0.8	1.0	0.0248	0.1207	0.5418	1.0054	1.4964	2.5268	2.9052
1.5	1.0	0.0133	0.0661	0.3247	0.6545	1.0468	1.9658	2.3234
1.2	1.0	0.0166	0.0820	0.3917	0.7679	1.1971	2.1605	2.5268
2.0	1.0	0.0100	0.0500	0.2528	0.5266	0.8697	1.7237	2.0678
0.5	2.0	0.2496	0.4950	0.9231	1.2104	1.4656	1.9558	2.1323
1.0	2.0	0.1827	0.3736	0.7289	0.9802	1.2104	1.6662	1.8336
0.8	2.0	0.2023	0.4097	0.7882	1.0514	1.2900	1.7576	1.9282
1.5	2.0	0.1516	0.3147	0.6291	0.8585	1.0725	1.5050	1.6662
1.2	2.0	0.1681	0.3461	0.6827	0.9243	1.1473	1.5929	1.7576
2.0	2.0	0.1326	0.2779	0.5645	0.7781	0.9802	1.3950	1.5512
0.5	1.5	0.1379	0.3634	0.8686	1.2489	1.5988	2.2811	2.5270
1.0	1.5	0.0891	0.2438	0.6268	0.9425	1.2489	1.8773	2.1107
0.8	1.5	0.1026	0.2779	0.6988	1.0359	1.3572	2.0047	2.2426
1.5	1.5	0.0687	0.1912	0.5099	0.7864	1.0639	1.6534	1.8773
1.2	1.5	0.0793	0.2187	0.5720	0.8701	1.1638	1.7754	2.0047
2.0	1.5	0.0570	0.1604	0.4376	0.6865	0.9425	1.5013	1.7174
0.5	0.8	0.0150	0.1099	0.6942	1.3884	2.0987	3.4993	3.9940
1.0	0.8	0.0064	0.0477	0.3516	0.8175	1.3884	2.6736	3.1526
0.8	0.8	0.0084	0.0625	0.4427	0.9828	1.6047	2.9356	3.4211
1.5	0.8	0.0038	0.0290	0.2262	0.5665	1.0340	2.2113	2.6736
1.2	0.8	0.0051	0.0381	0.2893	0.6967	1.2224	2.4632	2.9356
2.0	0.8	0.0027	0.0203	0.1631	0.4265	0.8175	1.8980	2.3434
0.5	2.5	0.3500	0.5902	0.9568	1.1876	1.3881	1.7684	1.9047
1.0	2.5	0.2758	0.4760	0.7953	1.0033	1.1876	1.5442	1.6738
0.8	2.5	0.2981	0.5107	0.8452	1.0608	1.2505	1.6150	1.7470
1.5	2.5	0.2391	0.4176	0.7096	0.9037	1.0777	1.4189	1.5442
1.2	2.5	0.2587	0.4490	0.7559	0.9577	1.1375	1.4873	1.6150
2.0	2.5	0.2157	0.3798	0.6528	0.8368	1.0033	1.3329	1.4548
0.5	3.0	0.4342	0.6608	0.9796	1.1725	1.3375	1.6472	1.7577
1.0	3.0	0.3588	0.5557	0.8417	1.0188	1.1725	1.4650	1.5705
0.8	3.0	0.3818	0.5881	0.8847	1.0670	1.2244	1.5227	1.6298
1.5	3.0	0.3199	0.5003	0.7671	0.9346	1.0812	1.3627	1.4650
1.2	3.0	0.3409	0.5302	0.8076	0.9804	1.1309	1.4186	1.5227
2.0	3.0	0.2946	0.4636	0.7168	0.8775	1.0188	1.2923	1.3921

Table 5 presents the numerical values of selected order statistics (percentiles) for the OW–HL distribution under various parameter combinations of λ and β . The results indicate that percentile values increase systematically with higher quantile levels, consistent with the distribution's positively skewed nature. Lower values of λ and β yield broader percentile spacing, reflecting heavier tails, whereas higher parameter values compressed the distribution, indicating lighter tails. These patterns confirmed the flexibility of the OW–HL distribution in capturing diverse data shapes and tail behaviours across parameter configurations.

3.3. Parameter Estimation

Let X_1, X_2, \dots, X_n be a random sample of size n from the OW-HL(λ, β) distribution with PDF

$$f_{OW-HL}(x; \lambda, \beta) = \frac{\lambda\beta}{2^\beta} e^x (e^x - 1)^{\beta-1} \exp\left\{-\lambda \left[\frac{e^x - 1}{2}\right]^\beta\right\}$$

Let $w_i = \frac{e^{x_i} - 1}{2}$, thus $f_{OW-HL}(x; \lambda, \beta) = \frac{\lambda\beta}{2^\beta} e^x (e^x - 1)^{\beta-1} \exp\{-\lambda w_i^\beta\}$. The likelihood function is given by:

$$\begin{aligned} L(\lambda, \beta) &= \prod_{i=1}^n f_{OW-HL}(x_i; \lambda, \beta) \\ &= \prod_{i=1}^n \frac{\lambda\beta}{2^\beta} e^{x_i} (e^{x_i} - 1)^{\beta-1} \exp\{-\lambda w_i^\beta\} \end{aligned} \quad (31)$$

and the log-likelihood is given by:

$$\ell(\lambda, \beta) = n \ln \lambda + n \ln \beta - n \beta \ln 2 + \sum_{i=1}^n x_i + (\beta - 1) \sum_{i=1}^n \ln(e^{x_i} - 1) - \lambda \sum_{i=1}^n w_i^\beta \quad (32)$$

The derivatives of the log-likelihood function with respect to λ and β are critical for finding the MLEs. The partial derivatives are given by Equations (33) and (34) as follows:

$$\frac{\partial \ell}{\partial \lambda} = \frac{n}{\lambda} - \sum_{i=1}^n w_i^\beta \quad (33)$$

$$\frac{\partial \ell}{\partial \beta} = \frac{n}{\beta} - n \ln 2 + \sum_{i=1}^n \ln(e^{x_i} - 1) - \lambda \sum_{i=1}^n w_i^\beta \ln w_i \quad (34)$$

Setting the partial derivatives equal to zero, we obtain the maximum likelihood equations given by Equations (35) and (36):

$$\frac{n}{\lambda} - \sum_{i=1}^n w_i^\beta = 0 \quad (35)$$

$$\frac{n}{\beta} - n \ln 2 + \sum_{i=1}^n \ln(e^{x_i} - 1) - \lambda \sum_{i=1}^n w_i^\beta \ln w_i = 0 \quad (36)$$

From the above, it is evident that the maximum likelihood equation with respect to λ provides a closed-form estimator once β is specified. In contrast, the equations for β involve nonlinear terms, making it impossible to obtain explicit analytical solutions. Consequently, the maximum likelihood estimates (MLEs) of the parameter vector $\xi = (\lambda, \beta)$ must be obtained numerically using standard iterative optimization techniques, such as the Newton–Raphson method or the Broyden–Fletcher–Goldfarb–Shanno (BFGS) algorithm.

4. Simulation Study

To implement the simulation study, we consider 1000 replications for each scenario. Six distinct parameter settings of the Odd Weibull–Half Logistic (OW–HL) distribution are chosen to provide a broad representation of different distributional shapes and behaviours: **Set I:** ($\lambda = 0.5, \beta = 1.0$) moderate scale with a light shape effect. **Set II:** ($\lambda = 1.0, \beta = 2.0$) baseline configuration. **Set III:** ($\lambda = 0.8, \beta = 1.5$) intermediate scale and shape, reflecting balanced hazard dynamics. **Set IV:** ($\lambda = 1.5, \beta = 0.8$) larger scale and smaller shape, often producing heavier tails. **Set V:** ($\lambda = 2.0, \beta = 3.0$) both scale and shape are large, highlighting heavier tail effects. **Set VI:** ($\lambda = 1.2, \beta = 2.5$) moderate scale with stronger shape influence, capturing complex hazard behaviour. The six parameter sets

were chosen to represent a broad range of distributional behaviours, from light- to heavy-tailed forms and simple to complex hazard patterns, ensuring a robust evaluation of the OW–HL distribution. For each parameter set, random samples of sizes $n = 50, 100, 100, 250, 500$ and 1000 are generated from the OW–HL distribution. Each generated dataset is fitted using the maximum likelihood estimation (MLE) procedure. Across all simulation replications, we compute the following performance metrics: bias, mean square error (MSE), average length (AL) and coverage probability (CP) of the estimates. The equations of these measures can be found in [40]. The performance metrics complement one another: bias captures systematic deviation, MSE reflects overall estimation accuracy, AL measures the precision of confidence intervals and CP evaluates their reliability. Together, they provide a comprehensive assessment of the efficiency and robustness of the estimation method.

Table 6 presents the simulation results of the OW–HL distribution for various parameter configurations and sample sizes. The results indicated that as the sample size increases, the mean estimates of both parameters (λ and β) converged to their true values, confirming the consistency of the maximum likelihood estimators. The biases and MSEs decrease steadily with larger samples, while the average lengths (ALs) of the confidence intervals become narrower, indicating greater estimation precision. The coverage probabilities (CPs) remained close to the nominal 95% level across all settings, demonstrating the reliability and stability of the estimation procedure. The simulation results confirmed the robustness and efficiency of the proposed OW–HL estimators in recovering the true parameters.

Table 6: Simulation results of the OW-HL distribution

Parameter		Mean Estimate	Bias		MSE		AL		CP			
λ	β		$\hat{\lambda}$	$\hat{\beta}$	λ	β	λ	β	λ	β		
0.5	1.0	50	0.5054	1.0288	0.0054	0.0288	0.0091	0.0156	0.3691	0.4467	0.9420	0.9390
		100	0.4980	1.0143	-0.0020	0.0143	0.0045	0.0075	0.2589	0.3109	0.9380	0.9400
		250	0.5001	1.0046	0.0000	0.0046	0.0017	0.0026	0.1643	0.1946	0.9560	0.944
		500	0.5015	1.0019	0.0015	0.0019	0.0008	0.0012	0.1164	0.1370	0.9560	0.9530
		1000	0.4998	1.0022	0.0002	0.0022	0.0004	0.0006	0.0821	0.0969	0.9540	0.9620
1.0	2.0	50	1.0244	2.0577	0.0244	0.0577	0.0250	0.062	0.5968	0.8933	0.9480	0.9390
		100	1.0020	2.0287	0.0020	0.0287	0.0109	0.0301	0.4140	0.6218	0.9580	0.9400
		250	1.0021	2.0092	0.0021	0.0092	0.0043	0.0105	0.2616	0.3891	0.9530	0.9440
		500	1.0037	2.0038	0.0037	0.0038	0.0021	0.0047	0.1852	0.2739	0.9530	0.9530
		1000	1.0009	2.0045	0.0009	0.0045	0.0011	0.0023	0.1306	0.1938	0.9520	0.9620
0.8	1.5	50	0.8154	1.5432	0.0154	0.0432	0.0174	0.0351	0.5039	0.6700	0.9460	0.9390
		100	0.7998	1.5215	-0.0002	0.0215	0.0080	0.0169	0.3513	0.4663	0.9560	0.9400
		250	0.8011	1.5069	0.0011	0.0069	0.0031	0.0059	0.2223	0.2919	0.9540	0.9440
		500	0.8028	1.5029	0.0028	0.0029	0.0015	0.0026	0.1574	0.2054	0.9600	0.9530
		1000	0.8003	1.5034	0.0003	0.0034	0.0008	0.0013	0.1111	0.1454	0.9490	0.9620
1.5	0.8	50	1.5536	0.8231	0.0536	0.0231	0.0567	0.0099	0.8674	0.3573	0.9510	0.9390
		100	1.5109	0.8115	0.0109	0.0115	0.0223	0.0048	0.5941	0.2487	0.9570	0.9400
		250	1.5058	0.8037	0.0058	0.0037	0.0092	0.0017	0.3738	0.1557	0.9520	0.9440
		500	1.5066	0.8015	0.0066	0.0015	0.0043	0.0007	0.2643	0.1096	0.9540	0.9530
		1000	1.5026	0.8018	0.0026	0.0018	0.0022	0.0004	0.1863	0.0775	0.9520	0.9620
2.0	3.0	50	2.0908	3.0865	0.0908	0.0865	0.1158	0.1404	1.2048	1.3400	0.9510	0.9390

		100	2.0234	3.0430	0.0234	0.0430	0.0430	0.0678	0.8155	0.9327	0.9560	0.940
		250	2.0108	3.0138	0.0108	0.0138	0.0180	0.0237	0.5109	0.5837	0.9440	0.9440
		500	2.010	3.0058	0.0100	0.0058	0.0081	0.0105	0.3607	0.4109	0.9630	0.9530
		1000	2.0047	3.0067	0.0047	0.0067	0.0041	0.0052	0.2541	0.2907	0.9570	0.9620
1.2	2.5	50	1.2350	2.5721	0.0350	0.0721	0.0352	0.0975	0.6974	1.1166	0.9470	0.9390
		100	1.2051	2.5359	0.0051	0.0359	0.0146	0.0471	0.4814	0.7772	0.9570	0.9400
		250	1.2034	2.5115	0.0034	0.0115	0.0059	0.0164	0.3037	0.4864	0.9510	0.9440
		500	1.2048	2.5048	0.0048	0.0048	0.0029	0.0073	0.2149	0.3424	0.9510	0.9530
		1000	1.2015	2.5056	0.00146	0.0056	0.0015	0.0036	0.1515	0.2423	0.9530	0.9620

Figure 10 presents the performance evaluation of maximum likelihood estimators for the OW–HL distribution parameters $\lambda = 1.0$, $\beta = 2.0$ across different sample sizes ($n = 50, 100, 250, 500, 1000$). The bias and mean squared error plots revealed rapid convergence of both estimators toward zero as sample size increases, confirming unbiasedness and improved precision with larger samples. The average confidence interval lengths (ALs) decrease steadily, indicating enhanced estimation efficiency, while the coverage probabilities (CPs) remained close to the nominal 95% level across all sample sizes (n), validating the reliability of the constructed confidence intervals. Collectively, the figure demonstrates that the MLEs for λ and β exhibited desirable asymptotic properties, achieving accurate and stable performance even at moderate sample sizes.

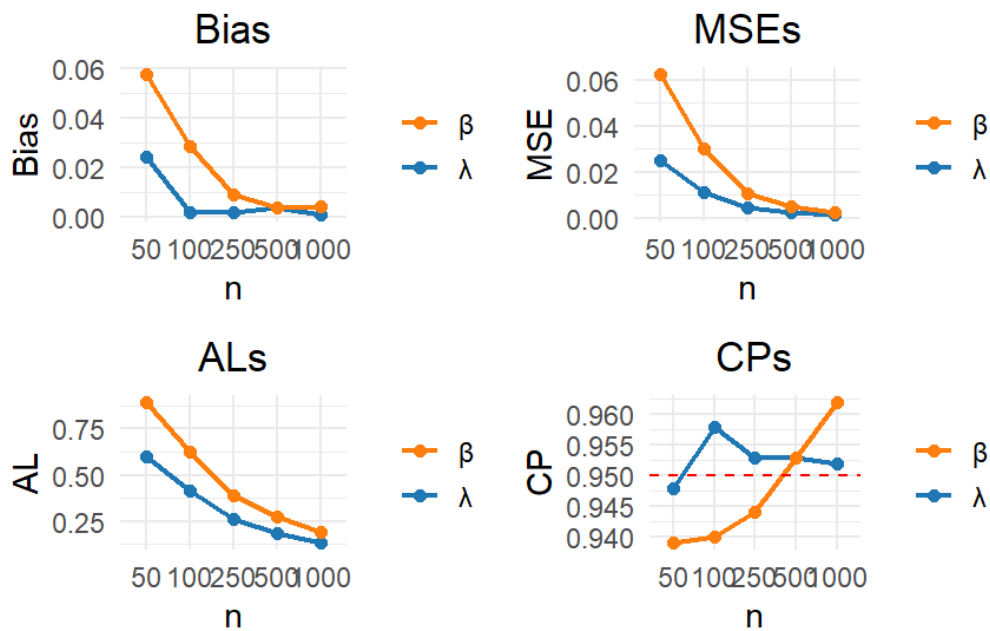


Figure 10: Plot of estimated Bias, MSEs, ALs, and CPs for the baseline Parameters True Values ($\lambda = 1.0, \beta = 2.0$)

5. Application

In this section, we demonstrate the practical utility of the proposed Odd Weibull–Half Logistic (OW–HL) distribution through applications to three real data sets. The analysis aimed to empirically validate the flexibility and effectiveness of the OW–HL model in capturing diverse data behaviors. To assess its performance, the OW–HL distribution is compared against several established and widely used competing models. This section first describes the characteristics of the selected data sets, followed by a presentation of the benchmark distributions considered for comparison. The methodology adopted for model fittings is then outlined, and finally, a comprehensive discussion of the empirical results is provided.

5.1. Data Description

Three widely referenced datasets were selected for their demanding distributional properties: glass fiber breaking strength with a 15 cm and 1.5 cm lengths and UK gas consumption (UKgas). Their complex structures pose challenges for conventional models, highlighting the necessity of flexible distributional approaches.

5.1.1. Glass Fiber Breaking Strength with a 15 cm Length (Data Set I)

This dataset contains breaking strength measurements of 15 cm glass fibers, originally collected by the UK National Physical Laboratory. It has been widely analyzed in statistical literature [7, 28, 41- 43]. The data sets are presented as follows: 0.37, 0.40, 0.70, 0.75, 0.80, 0.81, 0.83, 0.86, 0.92, 0.92, 0.94, 0.95, 0.98, 1.03, 1.06, 1.06, 1.08, 1.09, 1.10, 1.10, 1.13, 1.14, 1.15, 1.17, 1.20, 1.20, 1.21, 1.22, 1.25, 1.28, 1.28, 1.29, 1.29, 1.30, 1.35, 1.35, 1.37, 1.37, 1.38, 1.40, 1.40, 1.42, 1.43, 1.51, 1.53, 1.61.

5.1.2. Glass Fiber Breaking Strength with a 1.5 cm Length (Data Set II)

Similarly, we analyze a second dataset on the breaking strength of glass fibers from the same laboratory, but with a shorter fiber length of 1.5 cm. Also, this data set has been widely analyzed in statistical literature [28, 43, 44]. The complete dataset is presented below: 0.55, 0.93, 1.25, 1.36, 1.49, 1.52, 1.58, 1.61, 1.64, 1.68, 1.73, 1.81, 2.074, 1.04, 1.27, 1.39, 1.49, 1.53, 1.59, 1.61, 1.66, 1.68, 1.76, 1.82, 2.01, 0.77, 1.11, 1.28, 1.42, 1.5, 1.54, 1.6, 1.62, 1.66, 1.69, 1.76, 1.84, 2.24, 0.81, 1.13, 1.29, 1.48, 1.5, 1.55, 1.61, 1.62, 1.66, 1.7, 1.77, 1.84, 0.84, 1.24, 1.3, 1.48, 1.51, 1.55, 1.61, 1.63, 1.67, 1.7, 1.78, 1.89.

5.1.3. UK Gas consumption (UKgas) (Data Set III)

The UK gas dataset is a quarterly time series of UK gas consumption in millions of therms. The dataset extracted and presented below is available in the base R datasets package [45].

160.1, 129.7, 84.8, 120.1, 160.1, 124.9, 84.8, 116.9, 169.7, 140.9, 89.7, 123.3, 187.3, 144.1, 92.9, 120.1, 176.1, 147.3, 89.7, 123.3, 185.7, 155.3, 99.3, 131.3, 200.1, 161.7, 102.5, 136.1, 204.9, 176.1, 112.1, 140.9, 227.3, 195.3, 115.3, 142.5, 244.9, 214.5, 118.5, 153.7, 244.9, 216.1, 188.9, 142.5, 301.0, 196.9, 136.1, 267.3, 317.0, 230.5, 152.1, 336.2, 371.4, 240.1, 158.5, 355.4, 449.9, 286.6, 179.3, 403.4, 491.5, 321.8, 177.7, 409.8, 593.9, 329.8, 176.1, 483.5, 584.3, 395.4, 187.3, 485.1, 669.2, 421.0, 216.1, 509.1, 827.7, 467.5, 209.7, 542.7, 840.5, 414.6, 217.7, 670.8, 848.5, 437.0, 209.7, 701.2, 925.3, 443.4, 214.5, 683.6, 917.3, 515.5, 224.1, 694.8, 989.4, 477.1, 233.7, 730.0, 1087.0, 534.7, 281.8, 787.6, 1163.9, 613.1, 347.4, 782.8

Table 7: Descriptive Statistics of the Data Sets

Metrics	Data Set I	Data Set II	Data Set III
Mean	1.1300	1.5068	337.6306
Median	1.1600	1.5900	220.9000
Standard Deviation	0.2714	0.3241	251.3348
Variance	0.0736	0.1051	63169.1694
Skewness	-0.7936	-0.8999	1.2997
Kurtosis	3.5995	3.9238	3.9267
Coefficient of Variation (%)	24.0155	21.5105	74.4408
Minimum	0.3700	0.5500	84.8000
Maximum	1.6100	2.2400	1163.9000

Note: Data set I - Glass Fiber Breaking Strength with a 15 cm Length. Data set II: Glass Fiber Breaking Strength with a 1.5 cm Length Data set III: UKgas

The descriptive statistics in Table 7 reveal fundamentally different data profiles: both glass fiber datasets (I & II) exhibit left-skewness (-0.79, -0.90) and low variability (CV ~20-24%), characteristic of strength data. In stark contrast, the UKgas dataset (III) displays pronounced right-skewness (1.30) and high variability (CV 74.44%). Its inclusion was therefore designed as a stringent stress test. The successful fitting of the Odd Weibull-Half Logistic distribution across these divergent profiles effectively capturing both negative and positive asymmetry with varying dispersion, provides compelling evidence of its superior adaptability and flexibility over competing models.

5.2. Model Fitting and Comparative Analyses with Competing Distributions

The OW-HL distribution was fitted to the three datasets using the MLE method. For comparative assessment, Weibull distribution proposed by [46], Exponentiated Half Logistic (EHL) distribution proposed by [9], Exponentiated Weibull (EW) distribution proposed by [47], Log logistic (LL) distribution proposed by [48], generalized gamma (GG) distribution proposed by [49], Kumaraswamy Half Logistic (KuHL) distribution proposed by [50], Half Logistic (HL) distribution proposed by [51], exponential (E) distribution proposed by [52] and Lamac distribution proposed by [53] were also fitted to the same datasets. The adequacy of the fitted models was assessed using established goodness-of-fit statistics: the negative log-likelihood (LogLL), Akaike Information Criterion (AIC), Consistent Akaike Information Criterion (CAIC), Bayesian Information Criterion (BIC), and Hannan-Quinn Information Criterion (HQIC), where lower values indicate a preferable balance of fit and parsimony. This quantitative evaluation was supplemented by visual diagnostics, including probability density function (PDF) plots overlaid on data histograms and empirical cumulative distribution function (CDF) plots compared to their fitted theoretical counterparts. The results of this comprehensive analysis are presented below.

Table 8: Parameter Estimates and Goodness-of-Fit Statistics for data set I

Distribution	Parameter Estimates	LogLL	AIC	CAIC	BIC	HQIC
OW-HL	$\lambda = 0.5280$ $\beta = 3.0863$	-2.2544	8.5088	8.7878	12.1660	9.8788
Weibull	scale = 1.2296 shape = 5.1473	-3.3494	10.6988	10.9778	14.3561	12.0688
EW	$\alpha = 0.3935$ $\beta = 9.5923$ $\gamma = 1.3868$	-2.0813	10.1627	10.7341	15.6486	12.2178
GG	$\mu = 0.2633$ $\sigma = 0.1604$ Q = 1.6615	-2.0671	10.1342	10.7057	15.6202	12.1893
KuHL	scale = 4.5208 a = 5.1745 b = 31350.5093	-3.4125	12.8251	13.3965	18.3110	14.8801
LL	scale = 1.1339 shape = 6.8135	-9.1386	22.2771	22.5562	25.9344	23.6472
EHL	scale = 0.3116 $\alpha = 11.7571$	-13.7008	31.4016	31.6807	35.0589	32.7717
HL	$\varepsilon = 0.7425$	-43.5316	89.0633	89.1542	90.8919	89.7483

Exponential	rate = 0.885	-51.6220	105.2440	105.3349	107.0727	105.9290
Lomax	$\alpha = 95218.2113$	-51.6222	107.2445	107.5235	110.9018	108.6145
	$\beta = 107583.1687$					

Table 8 summarizes the parameter estimates and goodness-of-fit statistics for several competing models fitted to Glass Fiber Breaking Strength with a 15 cm Length (Data Set I). Among all the considered distributions, the proposed OW-HL model achieved the highest log-likelihood and the lowest AIC, CAIC, BIC, and HQIC values, indicating superior performance and best fit to the data. These results highlight the strong modeling capability and flexibility of the OW-HL distribution compared to other classical and generalized lifetime models.

Figure 11 compares the fitted PDFs of ten competing models against the empirical histogram of glass fiber breaking strength data (15 cm length). The OW-HL distribution (solid red line, ranked 1st) provides the closest fit, accurately capturing both the central peak and right tail. The Weibull, Exponentiated Half Logistic, and Exponentiated Weibull distributions show moderate fits, while others deviate notably from the empirical shape.

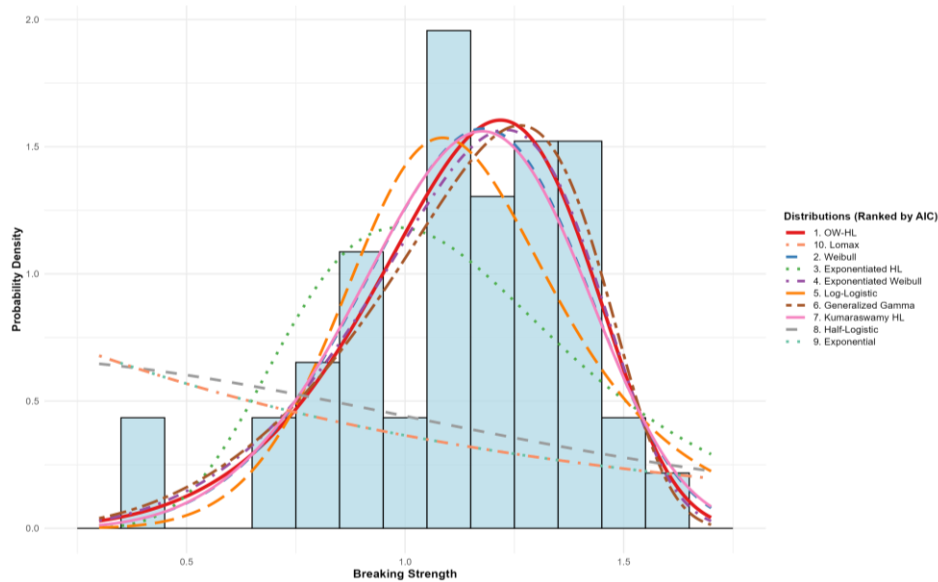


Figure 11: Fitted PDFs of the competing models for Data set I.

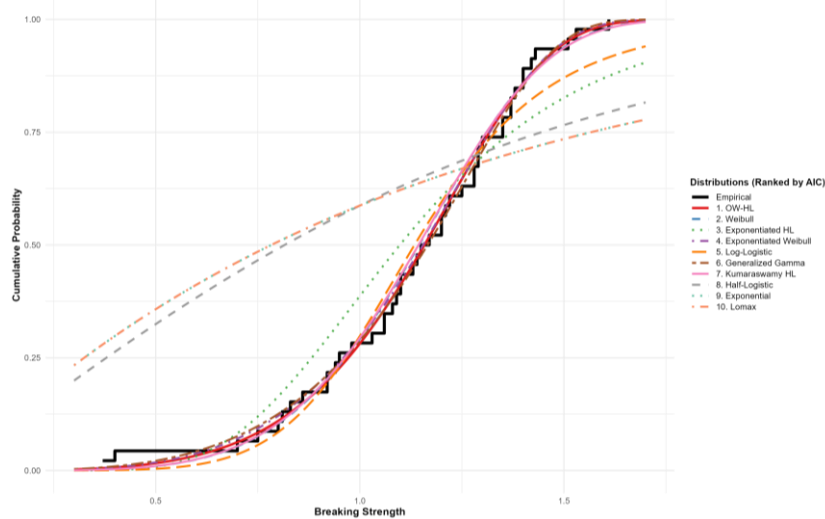


Figure 12: Fitted CDFs of the competing models for Data set I.

Figure 12 compares the fitted CDFs of ten competing models with the empirical CDF of the glass fiber breaking strength data (15 cm length). The OW–HL distribution (solid red line, ranked 1st) aligns almost perfectly with the empirical CDF across all quantiles, accurately capturing both tails and the central region. The Weibull, Exponentiated Half Logistic, and Exponentiated Weibull models follow reasonably well but show slight tail deviations. Other distributions diverge more noticeably.

Table 9: Parameter estimate and goodness of fit statistics for data set II

Distribution	Parameter Estimates	LogLL	AIC	CAIC	BIC	HQIC
OW-HL	$\lambda = 0.1179,$ $\beta = 2.9100$	-14.4022	32.8044	33.0044	37.0907	34.4902
Weibull	scale = 1.6281 shape = 5.7806	-15.2068	34.4137	34.6137	38.7000	36.0995
GG	$\mu = 0.5089$ $\sigma = 0.1637$ Q = 1.2703	-14.5876	35.1752	35.5820	41.6046	37.7039
EW	$\alpha = 0.6712$ $\beta = 7.2847$ $\gamma = 1.7181$	-14.6755	35.3510	35.7578	41.7804	37.8798
KuHL	scale = 4.9251 a = 5.8394 b = 38762.0799	-15.2844	36.5688	36.9755	42.9982	39.0975
LL	scale = 1.5262 shape = 7.926	-22.7900	49.5799	49.7799	53.8662	51.2657
EHL	scale = 0.3765 $\alpha = 17.1761$	-30.6227	65.2453	65.4453	69.5316	66.9311
HL	$\varepsilon = 0.9874$	-77.5031	157.0062	157.0718	159.1493	157.8491
Exponential	rate = 0.6636	-88.8303	179.6606	179.7262	181.8038	180.5035
Lomax	$\alpha = 47048.5749$ $\beta = 70879.2508$	-88.8310	181.6619	181.8619	185.9482	183.3477

Table 9 presents the parameter estimates and goodness-of-fit measures for several competing models fitted to Glass Fiber Breaking Strength with a 1.5 cm Length (Data Set II). The OW–HL distribution exhibited the highest log-likelihood and the lowest AIC, CAIC, BIC, and HQIC values among all the considered models. These results confirmed that the OW–HL model provides the best overall fit, demonstrating its superior flexibility and effectiveness in capturing the underlying structure of the data compared to traditional lifetime distributions.

Figure 13 compares fitted PDFs of ten competing models with the histogram of the 1.5 cm glass fiber breaking strength data (data II). The OW–HL distribution (solid red line, ranked 1st) provides the closest fit, accurately capturing the central peak and tail behaviour. The Weibull, Exponentiated Half Logistic, and Exponentiated Weibull models approximated the data moderately well but show slight deviations in peak height and tail shape, while the Lomax and other lower-ranked models exhibit clear mismatches.

Figure 14 compares the fitted CDFs of ten competing models with the empirical CDF for the 1.5 cm glass fiber breaking strength data. The OW–HL distribution (solid red line, ranked 1st) showed the closest agreement with the empirical CDF across all probability levels, accurately representing both the lower and upper tails as

well as the steep central rise. The Weibull, Exponentiated Half Logistic, and Exponentiated Weibull models follow the data reasonably well but displayed mild deviations in the tails, while the remaining distributions, including Lomax and Exponential, show clear mismatches and systematic bias.

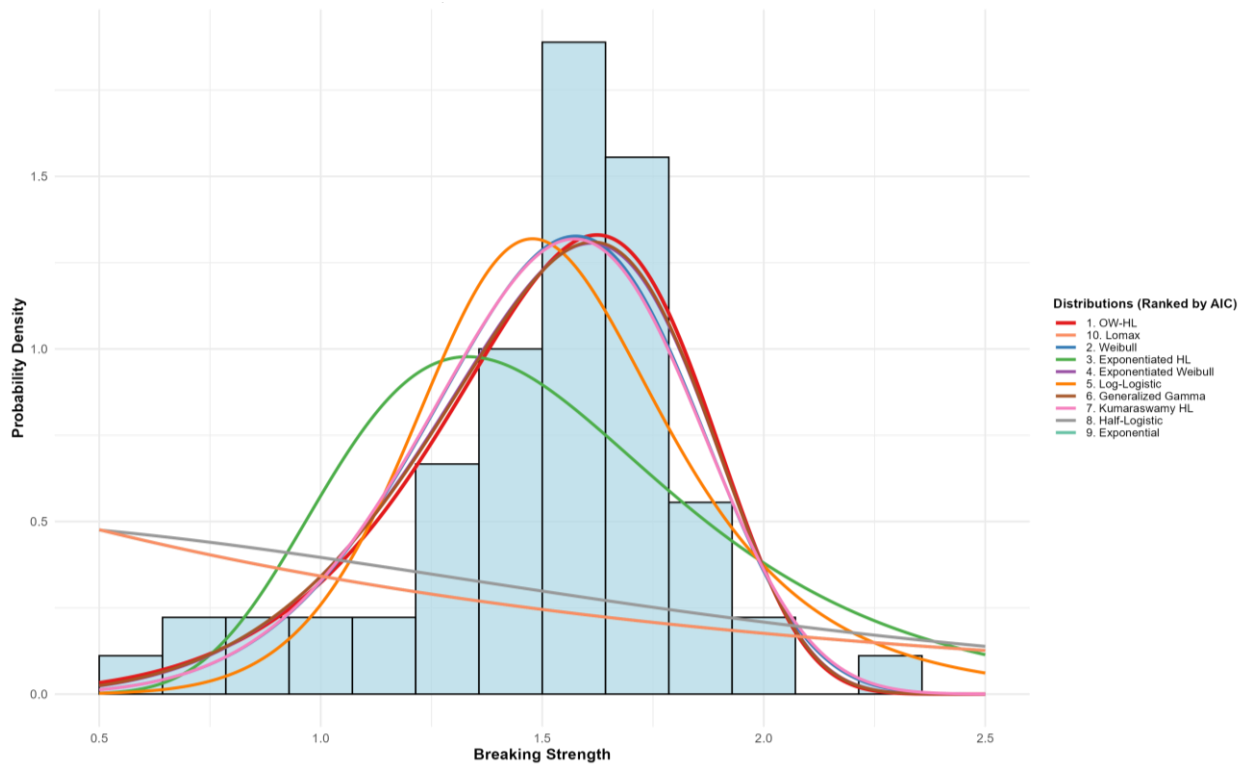


Figure 13: Fitted PDFs of the competing models for Data set II.

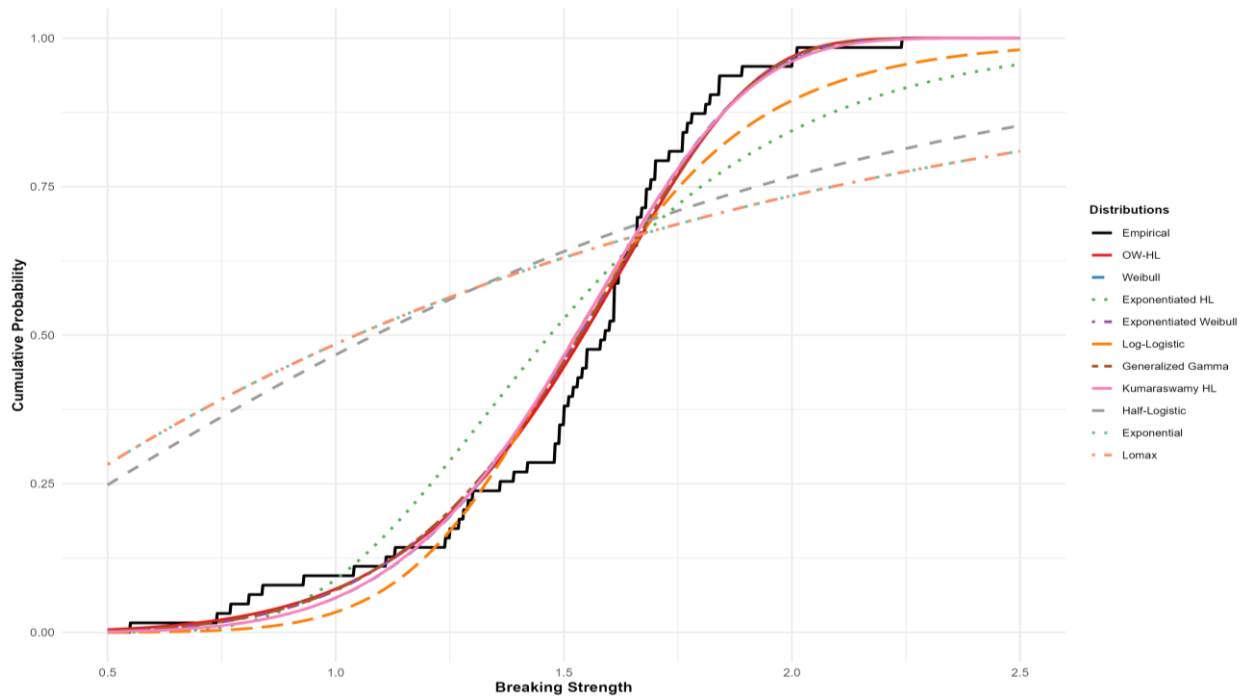


Figure 14: Fitted CDFs of the competing models for Data set II

Table 10: Parameter estimate and goodness of fit statistics for data set III

Distribution	Parameter Estimates	LogLik	AIC	AICc	BIC	HQIC
OW-HL	$\lambda = 0.0062$ $\beta = 1.2272$	34.2541	-64.5081	-64.3938	-59.1439	-62.3331
GG	$\mu = 5.3056$ $\sigma = 0.5995$ $Q = -0.8229$	-712.3930	1,430.7859	1,431.0167	1,438.8323	1,434.0484
EW	$\alpha = 312.9907$ $\beta = 0.2834$ $\gamma = 0.4169$	-712.6344	1,431.2689	1,431.4996	1,439.3153	1,434.5314
LL	scale = 254.9243 shape = 2.4372	-718.9431	1,441.8862	1,442.0005	1,447.2505	1,444.0612
EHL	scale = 177.8493 $\alpha = 1.7633$	-723.4875	1,450.9750	1,451.0893	1,456.3393	1,453.1500
Weibull	scale = 376.7901 shape = 1.4741	-724.7650	1,453.5300	1,453.6443	1,458.8943	1,455.7050
HL	scale = 236.6237	-730.9142	1,463.8284	1,463.8661	1,466.5105	1,464.9159
Exponential	rate = 0.0030	-736.7708	1,475.5417	1,475.5794	1,478.2238	1,476.6292
Lomax	$\alpha = 8110.11$ $\beta = 2738118.6301$	-736.7738	1,477.5477	1,477.6620	1,482.9120	1,479.7227
KuHL	scale = 1 a = 1.5 b = 1.5	-74,603.7570	149,213.5140	149,213.7448	149,221.5604	149,216.7765

Table 10 summarizes the parameter estimates and goodness-of-fit indices for the OW–HL and several competing models fitted to UKgas (Data Set III). The OW–HL distribution achieved the highest log-likelihood and the lowest AIC, AICc, BIC, and HQIC values, indicating the best overall fit. This result highlights the strong modeling capability and adaptability of the OW–HL distribution in capturing complex data patterns more effectively than existing lifetime models.

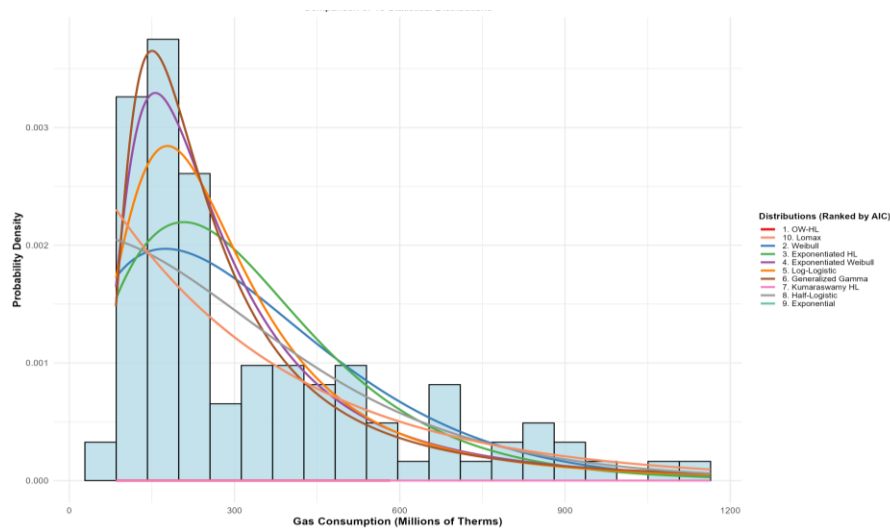


Figure 15: Fitted PDFs of the competing models for Data set III.

Figure 15 compares fitted PDFs of nine competing models with the histogram of UK quarterly gas consumption data. The data show strong right skewness with a sharp peak around 150–200 million therms and a long right tail. The OW–HL distribution (solid red line, ranked 1st) provides the closest fit, accurately capturing both the central peak and tail behaviour. Competing models such as Weibull, Exponentiated HL, and Exponentiated Weibull show moderate fits, while Lomax and other lower-ranked models fail to represent the peak or tail adequately.

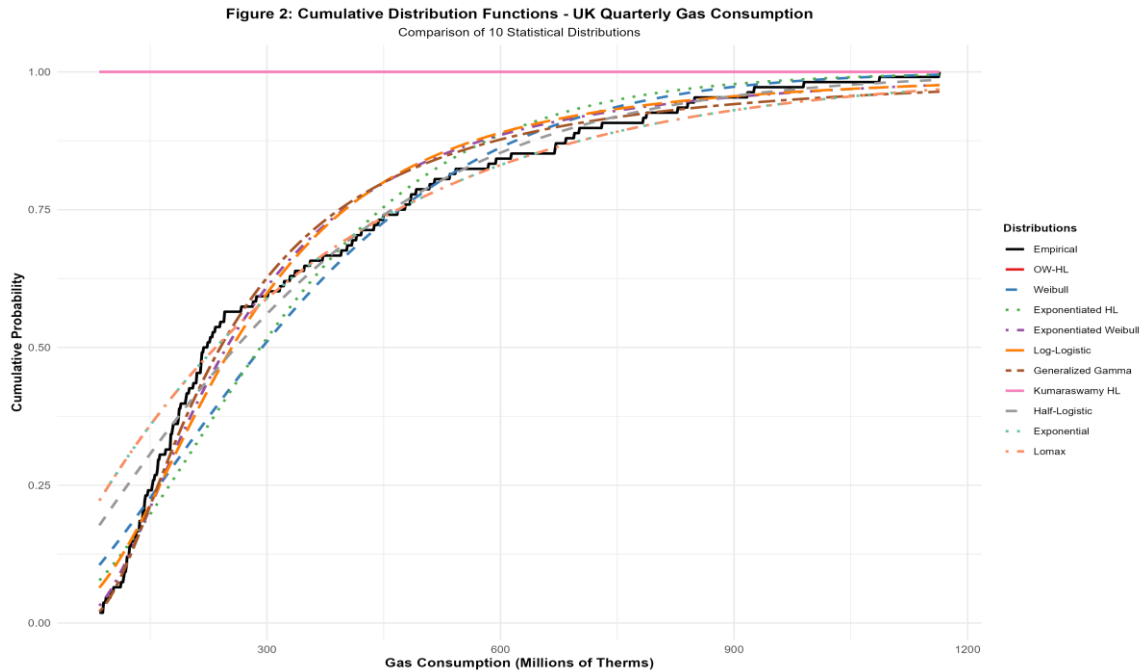


Figure 16: Fitted CDFs of the competing models for Data set III

Figure 16 compares the fitted CDFs of ten competing models with the empirical CDF of UK quarterly gas consumption. The empirical CDF rises steeply between 100 and 400 million therms, indicating concentrated mid-range consumption, followed by a gradual upper-tail increase. The OW–HL distribution (solid red line, ranked 1st) aligns almost perfectly with the empirical CDF, accurately capturing both the central accumulation and the extended right tail. Competing models such as Weibull, Exponentiated HL, and Exponentiated Weibull showed moderate fits but deviate in tail regions, while lower-ranked models exhibit substantial systematic errors. The close agreement of the OW–HL model across all quantiles underscores its superior fit and reliability for modelling energy consumption distributions and forecasting high-demand periods.

6. Conclusion

This study introduced and explored the OW-HL distribution, a new and flexible statistical model designed to capture a wide range of data behaviours, including skewness, kurtosis, and diverse hazard rate shapes. Through theoretical analysis, simulation experiments, and real data applications, the OW–HL distribution demonstrated superior performance over several well-established lifetime models such as the Weibull, Exponentiated Weibull, Log-Logistic, and Lomax distributions. The results revealed that the proposed model provides an excellent fit across datasets exhibiting light to heavy tails and monotonic as well as non-monotonic hazard structures. Simulation findings confirmed the consistency and efficiency of the maximum likelihood estimators, while empirical applications spanning reliability, materials science, and energy consumption data highlighted the OW–HL model’s robustness and adaptability for real-world data modelling and prediction. Future research may focus on extending the OW–HL framework to multivariate, regression, and censoring

contexts to enhance its applicability in survival and reliability studies. Potential avenues include developing Bayesian and robust estimation techniques, exploring information-theoretic and entropy-based optimization, and incorporating covariate effects through generalized linear or accelerated failure time formulations. Additionally, the use of the OW–HL distribution in machine learning pipelines, stochastic modelling, and risk analysis could be further investigated. These extensions would deepen the theoretical understanding of the model and expand its practical utility in complex data-driven disciplines such as biostatistics, engineering reliability, and financial risk management.

Author contributions: Conceptualization, G. K. Musa and Ibrahim Adamu Yunusa; Methodology, G. K. Musa; Writing—original draft, G. K. Musa; Writing—review and editing, Y. B. Usman and Ibrahim Adamu Yunusa.

Funding Statement: This research received no external funding.

Data Availability: The datasets generated and analyzed during this study are available from the corresponding author on reasonable request.

Acknowledgments: The authors are grateful to the reviewers for their expert feedback that strengthened this research paper.

Conflict of interest: The authors declare no conflict of interest.

References

- [1] J. F. Lawless, *Statistical Models and Methods for Lifetime Data*, 2nd ed. Hoboken, NJ, USA: Wiley, 2003.
- [2] W. Q. Meeker, L. A. Escobar, F. G. Pascual, Y. Hong, P. Liu, W. M. Falk, and B. Ananthasayanam, "Modern statistical models and methods for estimating fatigue-life and fatigue-strength distributions from experimental data," *arXiv preprint arXiv:2212.04550*, 2022. [Online]. Available: <https://arxiv.org/abs/2212.04550>
- [3] M. H. Tahir and G. M. Cordeiro, "Compounding of distributions: a survey and new generalized classes," *Journal of Statistical Distributions and Applications*, vol. 3, no. 1, p. 13, 2016.
- [4] N. Balakrishnan and A. Hassan, "Order statistics from the half-logistic distribution," *J. Stat. Plan. Inference*, vol. 27, no. 2, pp. 177–188, 1991.
- [5] S. Dey, I. Ghosh, and D. Kumar, "Alpha-Beta Skew Logistic Distribution," *Statistica*, vol. 76, no. 1, pp. 75–100, 2016.
- [6] G. M. Cordeiro, M. Alizadeh, and E. M. M. Ortega, "The Exponentiated Half-Logistic Family of Distributions," *Journal of Probability and Statistical Science*, vol. 14, no. 1, pp. 1–25, 2016.
- [7] M. Bourguignon, R. B. Silva, and G. M. Cordeiro, "The Weibull-G family of probability distributions," *J. Data Sci.*, vol. 12, no. 1, pp. 53–68, 2014.
- [8] B. S. Rao, S. Nagendram, and K. Rosaiah, "Exponential half logistic additive failure rate model," *Int. J. Sci. Res.*, vol. 3, no. 5, pp. 1–10, 2013.
- [9] G. M. Cordeiro, M. Alizadeh, and E. M. M. Ortega, "The exponentiated half-logistic family of distributions: Properties and applications," *J. Probab. Stat.*, vol. 2014, p. 864396, 2014. doi: 10.1155/2014/864396.
- [10] S. D. Krishnarani, "On a power transformation of half-logistic distribution," *Journal of Probability and Statistics*, vol. 2016, p. 2084236, 2016.

- [11] A. H. Soliman, M. A. E. Elgarhy, and M. Shakil, "Type II half logistic family of distributions with applications," *Pakistan Journal of Statistics and Operation Research*, pp. 245-264, 2017.
- [12] E. Altun, M. N. Khan, M. Alizadeh, G. Ozel, and N. S. Butt, "Extended half-logistic distribution with theory and lifetime data application," *Pak. J. Stat. Oper. Res.*, pp. 319-331, 2018.
- [13] A. F. Samuel and O. A. Kehinde, "A study on transmuted half logistic distribution: Properties and application," *Int. J. Stat. Distrib. Appl.*, vol. 5, no. 3, p. 54, 2019.
- [14] A. M. Almarashi, M. M. Badr, M. Elgarhy, F. Jamal, and C. Chesneau, "Statistical inference of the half-logistic inverse Rayleigh distribution," *Entropy*, vol. 22, no. 4, p. 449, 2020. doi: 10.3390/e22040449.
- [15] A. Olapade, "The type I generalized half logistic distribution," *J. Iran. Stat. Soc.*, vol. 13, no. 1, pp. 69-82, 2022.
- [16] B. Oluyede and T. Moakofi, "Type II exponentiated half-logistic-Gompertz Topp-Leone-G family of distributions with applications," *Central European Journal of Economic Modelling and Econometrics*, no. 4, pp. 415-461, 2022.
- [17] A. Gul, A. J. Sandhu, M. Farooq, M. Adil, Y. Hassan, and F. Khan, "Half logistic-truncated exponential distribution: Characteristics and applications," *PLoS One*, vol. 18, no. 11, p. e0285992, 2023.
- [18] A. Al-Adilee and W. Al-Shemmari, "Generalized half-logistic distribution using linear regression model," *Mathematics and Statistics*, vol. 11, no. 6, pp. 936-942, 2023.
- [19] A. Barbiero and A. Hitaj, "Discrete half-logistic distributions with applications in reliability and risk analysis," *Ann. Oper. Res.*, vol. 340, no. 1, pp. 27-57, 2024. doi: 10.1007/s10479-024-06145-9.
- [20] A. A. Ogunde, S. Dutta, and E. M. Almetawally, "Half logistic generalized Rayleigh distribution for modeling hydrological data," *Ann. Data Sci.*, 2024, Advance online publication. doi: 10.1007/s40745-024-00540-5.
- [21] B. Makubate, F. Chipepa, B. Oluyede, and G. Moagi, "The Marshall-Olkin-exponentiated half logistic-G family of distributions: model, properties and applications," *J. Stat. Manag. Syst.*, vol. 27, no. 7, pp. 1243-1259, 2024. doi: 10.47974/JSTS-1275.
- [22] Y. Zheng, T. Ye, and W. Gui, "Parameter Estimation of Inverted Exponentiated Half-Logistic Distribution under Progressive Type-II Censored Data with Competing Risks," *Amer. J. Math. Manag. Sci.*, vol. 43, no. 1, pp. 21-39, 2024. doi: 10.1080/01966324.2023.2253896.
- [23] A. A. Adepoju, S. S. Abdulkadir, D. Jibasen, and J. S. Olumoh, "A Type I Half Logistic Topp-Leone Inverse Lomax distribution with Applications in Skinfolde Analysis," *Reliability: Theory & Appl.*, vol. 19, no. 1, pp. 618-630, 2024.
- [24] S. Chamunorwa, B. Oluyede, T. Moakofi, and F. Chipepa, "The Type II Exponentiated Half Logistic-Gompertz-G Power Series Class of Distributions: Properties and Applications," *Stat., Optim. & Inf. Comput.*, vol. 12, no. 2, pp. 381-399, 2024.
- [25] M. Genç and Ö. Özbilen, "Transmuted unit exponentiated half-logistic distribution and its applications," *Ordu Üniversitesi Bilim ve Teknoloji Dergisi*, vol. 14, no. 2, pp. 249-260, 2024.
- [26] M. Hashempour and M. Alizadeh, "A new two-parameter extension of half-logistic distribution: Properties, applications and different method of estimations," *Thailand Statistician*, vol. 22, no. 3, pp. 720-735, 2024.
- [27] J. S. Kamnge and M. Chacko, "Half logistic exponentiated inverse Rayleigh distribution: Properties and application to life time data," *PLoS ONE*, vol. 20, no. 1, p. e0310681, 2025. doi: 10.1371/journal.pone.0310681.

- [28] A. A. Suleiman, H. Daud, A. G. Usman, S. I. Abba, M. Othman, and M. Elgarhy, "A new two-parameter half-logistic distribution with numerical analysis and applications," *J. Stat. Sci. Comput. Intell.*, vol. 1, no. 2, pp. 1–15, 2025.
- [29] A. S. Hassan, N. Alsadat, M. Elgarhy, L. P. Sapkota, O. S. Balogun, and A. M. Gemeay, "A novel asymmetric form of the power half-logistic distribution with statistical inference and real data analysis," *Electron. Res. Arch.*, vol. 33, no. 2, pp. 791–825, 2025. doi: 10.3934/era.2025037.
- [30] M. Genç and Ö. Özbilen, "Sine unit exponentiated half-logistic distribution: Theory, estimation, and applications in reliability modeling," *Mathematics*, vol. 13, no. 11, p. 1871, 2025.
- [31] A. Alzaatreh, C. Lee, and F. Famoye, "A new method for generating families of continuous distributions," *Metron*, vol. 71, no. 1, pp. 63–79, 2013.
- [32] C. Lee, F. Famoye, and A. Alzaatreh, "Methods for generating families of univariate continuous distributions in the recent decades," *Journal of Statistical Distributions and Applications*, vol. 1, Dec. 2013, Art. no. 3.
- [33] N. Eugene, C. Lee, and F. Famoye, "Beta-normal distribution and its applications," *Commun. Stat. - Theory Methods*, vol. 31, no. 4, pp. 497–512, 2002.
- [34] G. M. Cordeiro and M. de Castro, "A new family of generalized distributions," *J. Stat. Comput. Simul.*, vol. 81, no. 7, pp. 883–898, 2011.
- [35] J. P. Klein and M. L. Moeschberger, *Survival Analysis: Techniques for Censored and Truncated Data*, 2nd ed. New York, NY, USA: Springer, 2003. doi: 10.1007/b97377.
- [36] D. G. Kleinbaum and M. Klein, *Survival Analysis: A Self-Learning Text*, 3rd ed. New York, NY, USA: Springer, 2012. doi: 10.1007/978-1-4419-6646-9.
- [37] D. Collet, *Modelling Survival Data in Medical Research*, 3rd ed. Boca Raton, FL, USA: CRC Press, 2015. [Online]. Available: <https://books.google.co.zw/books?id=Okf7CAAAQBAJ>
- [38] N. U. Nair, P. G. Sankaran, and N. Balakrishnan, *Quantile-Based Reliability Analysis*. Cham, Switzerland: Birkhäuser, 2022. doi: 10.1007/978-3-031-01352-5.
- [39] G. Casella and R. L. Berger, *Statistical Inference*, 2nd ed. Pacific Grove, CA, USA: Duxbury Press, 2002.
- [40] G. M. Cordeiro, M. Alizadeh, G. Ozel, B. Hosseini, E. M. M. Ortega, and E. Altun, "The generalized odd log-logistic family of distributions: properties, regression models and applications," *J. Stat. Comput. Simul.*, vol. 87, no. 5, pp. 908–932, 2017.
- [41] R. I. Smith and J. C. Naylor, "A comparison of maximum likelihood and Bayesian estimators for the three-parameter Weibull distribution," *Appl. Stat.*, vol. 36, no. 3, pp. 358–369, 1987. doi: 10.2307/2347795.
- [42] P. E. Oguntunde, M. A. Khaleel, M. T. Ahmed, A. O. Adejumo, and O. A. Odetunmibi, "A new generalization of the Lomax distribution with increasing, decreasing and constant failure rate," *Model. Simul. Eng.*, vol. 2017, p. 6043169, 2017. doi: 10.1155/2017/6043169.
- [43] A. A. Abdullahi, A. A. Suleiman, A. I. Ishaq, A. Usman, and A. Suleiman, "The Maxwell–exponential distribution: Theory and application to lifetime data," *J. Stat. Model. & Analytics (JOSMA)*, vol. 1, no. 2, pp. 68–83, 2021.
- [44] A. I. Ishaq and A. A. Abiodun, "The Maxwell-Weibull Distribution in Modeling Lifetime Datasets," *Ann. Data Sci.*, vol. 7, pp. 639–662, 2020.
- [45] R Core Team, *R: A Language and Environment for Statistical Computing*. Vienna, Austria: R Foundation for Statistical Computing, 2024. [Online]. Available: <https://www.R-project.org/>
- [46] W. Weibull, "A statistical distribution function of wide applicability," *J. Appl. Mech.*, vol. 18, no. 3, pp. 293–297, 1955.

- [47] G. S. Mudholkar and D. K. Srivastava, "Exponentiated Weibull family for analyzing bathtub failure-rate data," *IEEE Trans. Rel.*, vol. 42, no. 2, pp. 299–302, 1993. doi: 10.1109/24.229504.
- [48] M. M. Shoukri, I. U. M. Mian, and D. S. Tracy, "Sampling properties of estimators of the log-logistic distribution with application to Canadian precipitation data," *Can. J. Stat.*, vol. 16, no. 3, pp. 223–236, 1988. doi: 10.2307/3314729.
- [49] E. W. Stacy, "A generalization of the gamma distribution," *Ann. Math. Stat.*, vol. 33, no. 3, pp. 1187–1192, 1962. doi: 10.1214/aoms/1177704481.
- [50] M. A. Khaleel, P. E. Oguntunde, M. T. Ahmed, H. B. Asmai, and N. A. Ibrahim, "The Kumaraswamy half logistic distribution: Properties and applications," *J. Reliab. Stat. Stud.*, vol. 13, no. 1, pp. 1–22, 2020.
- [51] N. Balakrishnan, "Order statistics from the half logistic distribution," *J. Stat. Comput. Simul.*, vol. 20, no. 4, pp. 287–309, 1985. doi: 10.1080/00949658508810804.
- [52] B. Epstein, "The exponential distribution and its role in life testing," *Ind. Qual. Control*, vol. 17, no. 4, pp. 2–7, 1960.
- [53] K. S. Lomax, "Business failures: Another example of the analysis of failure data," *J. Amer. Stat. Assoc.*, vol. 49, no. 268, pp. 847–852, 1954. doi: 10.1080/01621459.1954.10501239.



Disclaimer/Publisher's Note: The views, opinions, and content expressed in all articles are solely those of the respective author(s) and contributor(s) and do not necessarily reflect those of the JSSCI, its editors, or the publisher. JSSCI and its editorial team assume no responsibility for any harm or damage resulting from the use of information, methods, or products mentioned in the publication.